MECHANICAL ENGINEERING | PHYSICS | PRESERVATION OF THE ARCHITECTURAL HERITAGE | STRUCTURAL, SEISMIC AND GEOTECHNICAL ENGINEERING | URBAN PLANNING, DESIGN AND POLICY | AEROSPACE ENGINEERING | ARCHITECTURE, BUILT ENVIRONMENT AND CONSTRUCTION ENGINEERING | ARCHITECTURAL, URBAN AND INTERIOR DESIGN | BIOENGINEERING | DATA ANALYTICS AND DECISION SCIENCES | DESIGN | ELECTRICAL ENGINEERING | ENERGY AND NUCLEAR SCIENCE AND TECHNOLOGY | ENVIRONMENTAL AND INFRASTRUCTURE ENGINEERING | INDUSTRIAL CHEMISTRY AND CHEMICAL ENGINEERING | INFORMATION TECHNOLOGY | MANAGEMENT ENGINEERING | MATERIALS ENGINEERING | MATHEMATICAL MODELS AND METHODS IN ENGINEERING

PhD Yearbook | 2025

Chair:
Prof. Salvatore Stagira

DOCTORAL PROGRAM IN PHYSICS

The Doctoral Program in Physics at Politecnico di Milano aims at attracting bright students with good scientific background and clear interest towards development and applications of new ideas and technologies. It offers a wide range of opportunities in the fields of advanced applied physics, such as photonics and optoelectronics (lasers, ultrafast optics), biomedical optics (optical tomography), vacuum technologies (thin film depositions), material technologies (microelectronics and nanotechnologies, micromechanical processing), and advanced instrumentation (electronic and atomic microscopy, nuclear magnetic resonance).

Scientific education and training to develop general research abilities in all areas of applied physics is increasingly needed by advanced technological companies. Through a general education in the basic areas of applied physics and a specific knowledge in condensed matter physics, as well as optics and lasers, the PhD Program aims at the development of an experimental approach to problem solving techniques and at the attainment of a high level of professional qualification.

The Doctoral Program has strongly experimental character. The contents are strictly related to the research activities carried out in the laboratories at the Department of Physics. They can be divided into two main areas:

a) Condensed Matter Physics, including photoemission; spin-resolved electronic spectroscopy; magneto-optics; X ray diffraction; magnetic nanostructures for spintronics; synchrotron radiation spectroscopy, positron spectroscopy, semiconductor nanostructures.
b) Photonics and Quantum Electronics, including ultrashort light pulse generation and applications; UV and X optical harmonics generation; biomedical applications of lasers; diagnostics for works of art; laser applications in optical communications; time domain optical spectroscopy and diagnostic techniques.

All research activities rely on advanced experimental laboratories located at Politecnico di Milano (Milano-Leonardo Campus and Como Campus) and are performed in collaboration with several international Institutions. Consistent effort is devoted to experimental research, development of innovative approaches and techniques, and design of novel instrumentation.

The educational program can be divided into three parts: 1) Courses specifically designed for the PhD program as well transdisciplinary courses; 2) Activities pertaining to more specific disciplines which will lay the foundation for the research work to be carried out during the Doctoral Thesis; 3) Doctoral Thesis. The thesis work is the major activity of the Program. It has a marked experimental character and will be carried out in one or more laboratories at the Department of Physics.
The students are also encouraged to perform part of their thesis work in laboratories of other national or foreign Institutions. Collaborations that may involve the PhD students are presently active with several national and international research and academic Institutions, such as: ETH-Zürich, EPL-Lausanne, Lund Institute of Technology, University of Paris-Sud, Ecole Polytechnique-Paris, University of Berkeley, University of Cambridge, University College London, Massachusetts Institute of Technology, Harvard University, European Space Agency, ENEA, Elettra-Ts, PSI-Villigen, Agenzia Spaziale Italiana, European Synchrotron Radiation Facility (ESRF-Grenoble), IFN-CNR, IIT–Istituto Italiano di Tecnologia.

At present, the number of students in the three-year course is 120.

The PhD Program Faculty, who takes care of organizing and supervising teaching and research activities, consists of members (listed here below), who are all highly qualified and active researchers covering a wide spectrum of research fields. This ensures a continuous updating of the PhD Program and guarantees that the students are involved in innovative research work.

FAMILY NAME	FIRST NAME	POSITION*
BERTACCO	RICCARDO	FP
BRAMBILLA	ALBERTO	AP
CAIRONI	MARIO	ST
CERULLO	GIULIO	FP
CICCACCI	FRANCO	FP
COMELLI	DANIELA	AP
CRESPI	ANDREA	AP
CUBEDDU	RINALDO	FP
DALLERA	CLAUDIA	FP
D'ANDREA	COSIMO	FP
DELLA VALLE	GIUSEPPE	FP
DUÒ	LAMBERTO	FP
FARINA	ANDREA	ST
FINAZZI	MARCO	FP
GAMBETTA	ALESSIO	AP
GHIRINGHELLI	GIACOMO	FP
ISELLA	GIOVANNI	FP
LANZANI	GUGLIELMO	FP
LAPORTA	PAOLO	FP
MARANGONI	MARCO	FP
MORETTI	MARCO	AP
NISOLI	MAURO	FP
PETTI	DANIELA	AP
PICONE	ANDREA	AP
POLLI	DARIO	FP
STAGIRA	SALVATORE	FP
TARONI	PAOLA	FP
TORRICELLI	ALESSANDRO	FP
VIRGILI	TERSILLA	ST
ZANI	MAURIZIO	AP

*Position: FP = Full Professor; AP = Associate Professor; ST = Scientist.

LOW-VOLTAGE, SECONDARY ELECTRON EMISSION SPECTROMICROSCOPY IN A CONTROLLED ULTRA-HIGH VACUUM ENVIRONMENT

Mehr Abbas Kosari - Supervisor: Alberto Tagliaferri

Investigating materials' local electronic/structural characteristics (in atomic scale) over depth from the surface to near-surface (~1-5 nm) is crucial in many applications ranging from nano-scale material mapping to local quantum state characterization. One of the potentially powerful techniques in this area is scanning electron microscopy (SEM) joined with secondary electron emission spectroscopy (SEES), in which a focused electron beam with high lateral spatial resolution (<few nm) extracts spectral information originating from the energy and angle distributions of the electrons emitted from a surface. In SEM, when the accelerating voltage reduces to low values (<3 kV), a higher portion of generated low-energy secondary electrons (SEs) have the chance to escape the surface without undergoing a collision. Moreover, fine structures appear on the material's spectral low-energy (<50 eV) function (Fig.1). The physics underlying this energy fine structure remains somewhat poorly understood. This is primarily due to the difficulty in extracting it from the extensive background associated with the SEs generated by a cascade of electron collisions. However, the detected fine structure reveals the role of the local electronic structure at the surface, involving the occupied/unoccupied quantum states near the Fermi level and the local work function. In the literature, this fine structure has been associated with the density of states (DOS) of the electronic band structures [Han, W., et al., Sci Rep 10, 22144 (2020)], which is more evident in crystalline materials, such as Highly oriented pyrolytic graphite (HOPG). Notwithstanding, the models proposed so far cannot picture the phenomena, and the experimental data lacks reproducibility.

In this work, we designed and simulated a new electron optics setup to exploit our Scanning Auger microscope (SAM) for recording low-energy electron (<50 eV) spectra.

The energy analysis of low-energy electrons was enabled by orienting the normal to the sample surface towards the energy analyzer entrance while applying a negative voltage to the specimen (Fig.2). The entrance optics enhanced the analyzer transmission and mitigated the strength of its background signal. The spectral performances were carefully characterized, with a relative energy resolution better than 6.5%, measured at the 15-30 eV energy range.

The experimental results on materials such as Cr, W, Au, Ta, MOS2, and HOPG show a contrast based on the overall line shape of the spectra, with trends predicted by a model combining the work function of the sample surface and the classical SE emission model by Chung-Everhart. The results also stress the need for an extension of the model for low accelerating voltages (< 3 kV), where the fine structure emerges. Accordingly, we focused on measuring and modeling this SE fine structure to extract the precious and unexploited DOS information on the sample surface. The experimental data show a relevant correlation with the DOS of the above materials, as found in the literature. We propose an analytical relationship between the spectral fine structure and the surface/near-surface DOS using the Fermi Golden rule and perturbation theory.

HOPG surface is a prototypical benchmark for evaluating the technique due to its surface stability, large energy valence band, and sharp DOS structure. Fig. 3 compares the experimental measurements and the spectral function predicted by our model from ab initio calculated DOS, showing a good agreement.

We conclude that our experimental approach and model show the potential to provide information about localized electronic structures of material surfaces. Future perspective applications include studying the dynamics of surface changes in an ultra-high vacuum environment, impacting photoelectrochemistry to photocathode characterization. For instance, the localized dynamics of a photocatalytic chemical reaction in the presence of a solid electrolyte can be studied by time-resolved SEES.

To reach these achievements, one should face several challenges. To thoroughly investigate the SE emission behavior, they should have a standard calibrated analyzer for low energies without distortion and background emission. Furthermore, the dose-dependent surface contamination and charging should be controlled and corrected during the measurement and data treatment. To this end, we propose a hemispherical lens design that can bring the position of the real and virtual sources as close as possible when negatively biasing the specimens. Distortionless SE acceleration can offer a short-term solution to enhance the performance of the conventional SAMs for SEES.

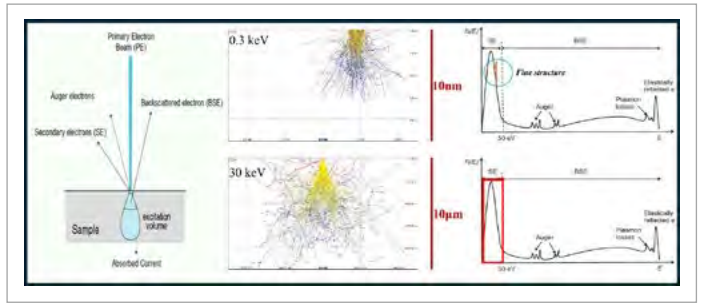

Fig.1 - Schematic diagram of signals generated when a focused electron beam impinges on the sample in SEM (left). 2D Montecarlo simulations of the electron interaction inside a solid (MOS2) when the primary beam energies are 0.3 keV (middle up) and 30 keV (middle down); Red trajectories represent backscattered electrons. Exemplary spectra acquired in SAM at low (right up) and high (right down) primary beam energies; the low energy part is labeled as the SE region.

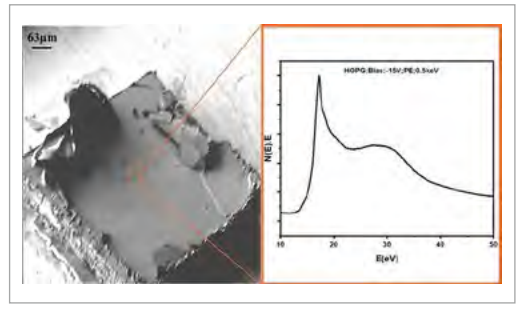

Fig.2 - SEM micrograph of the HOPG sample used in this study (left) and the spectrum acquired at the region of interest. The applied bias and the primary beam energy were -15 V and 0.5 keV, respectively.

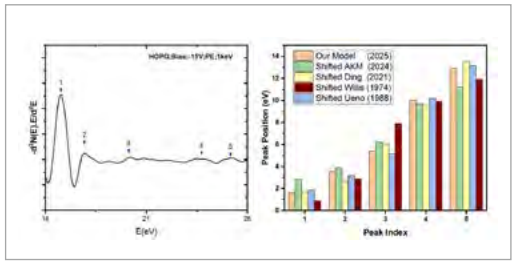

Fig.3 - Peak index/positions of our experimental data on HOPG, obtained by the minus second derivative of the signal taken at 1 keV (left). The bars compare the expected peak positions of HOPG by the model we proposed (in orange) and the experimental peaks we acquired (in green). Shifted experimental peaks reported in the literature are also plotted.

CONDUCTIVE THIOPHENE-BASED FIBERS ASSEMBLED BY LIVING CELLS AS NOVEL BIOELECTRONIC MATERIALS

Ludovico Aloisio – Supervisor: Guglielmo Lanzani

The ability of molecules to self-assemble into ordered structures supports many biological and synthetic systems, leading to functional materials with unique mechanical, optical, and electronic properties. Inspired by these natural processes, synthetic self-assembling materials have been developed to mimic or complement biological structures, with applications ranging from drug delivery to bioelectronics. In particular, conductive molecular assemblies have gained attention for their potential to integrate with biological tissues, offering new strategies for modulating cellular behavior and restoring lost functions. Self-assembled conductive fibers represent a promising approach for interfacing with biological systems, offering potential applications in bioelectronics and cellular communication.

One class of materials that has recently gained attention for its potential in bioelectronics is DTTO fibers. DTTO fibers stand out due to their intrinsic conductivity and ability to form within cellular environments, potentially acting as synthetic analogs of biological structures like gap junctions. Gap junctions are specialized intercellular connections that allow direct electrical and metabolic communication between adjacent cells. The ability of DTTO fibers to self-assemble inside cells without requiring external templates or scaffolds makes them particularly intriguing for interfacing with biological systems. This capability is advantageous because it allows for the creation of functional materials that are not only electrically conductive but also compatible with the dynamic environments inside living cells. Understanding the self-assembly process of these fibers is critical for optimizing their functional properties and leveraging them for bioelectronic applications.

In this thesis, the formation of conductive DTTO fibers within cells, their structural and electronic properties, and their ability to mediate electrical signal propagation between otherwise disconnected cells were investigated. Time-resolved photoluminescence (TRPL) measurements provided crucial insights into the self-assembly process of the fibers, confirming that they form through the molecular organization of DTTO molecules into crystalline structures. The ability to observe this process in real-time allowed for a deeper understanding of how these fibers form, which is essential for optimizing their electronic properties. Additionally, pump-probe spectroscopy provided further evidence of charge delocalization along the fibers, suggesting their potential for efficient charge transport across extended lengths. These findings prompted an extensive characterization of the fibers' electronic properties, highlighting their potential to facilitate efficient charge transport, which is crucial for their role as bioelectronic interfaces. The molecular packing within the fibers was found to be distinct from other types of DTTO assemblies, resulting in improved electronic performance. This observation is significant because it demonstrates that the self-assembly process can be tuned to optimize the electronic properties of the fibers. By understanding the factors that influence molecular packing, it may be possible to further enhance the conductivity and mechanical properties of the fibers, thus increasing their efficacy as bioelectronic interfaces. These improvements could be critical in applications where efficient signal propagation and mechanical flexibility are required, such as in neural interfaces or tissue engineering.

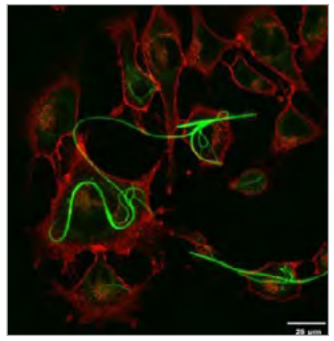

Fig.1 - Laser Scanning Confocal Microscopy images of C2C12 cells with DTTO fibers. Cells were stained with CellMask DeepRed right before confocal imaging to visualize the plasma membrane (red).

To assess the potential application of DTTO fibers as artificial gap junctions, the role of these fibers in facilitating intercellular communication in HEK-293T cells was investigated. Gap junctions are essential for direct electrical and metabolic coupling between cells, and their absence can disrupt coordinated cellular functions. The ability to restore electrical connectivity between cells is particularly important in excitable cells, such as neurons and cardiomyocytes, where precise electrical coupling is necessary for proper tissue function. Patch clamp measurements demonstrated that in the presence of DTTO fibers, the depolarization signal between two adjacent cells was restored, even when natural gap junctions were pharmacologically blocked. This is particularly notable because it indicates that the DTTO fibers can effectively bridge the electrical gap between disconnected cells, restoring the coordinated electrical behavior that is vital for normal cellular function. Furthermore, the amplitude of the signal transmission was comparable to that observed in healthy cells, further suggesting that the fibers can facilitate efficient electrical communication between cells.

A key aspect of this study was the time delay analysis of signal propagation between cells. This analysis indicated a resistive rather than capacitive behavior, confirming efficient charge transport across the fibers. This property is particularly relevant in the context of excitable cells, where precise timing and amplitude of electrical signals are required for proper function. In neurons, for instance, an action potential requires a membrane depolarization threshold to trigger propagation. In cells with impaired communication, the signal transduction was insufficient to reach this threshold, highlighting the lack of effective communication between the cells. However, in the presence of DTTO fibers, the signal propagation was restored to a level that would allow action potential initiation. This finding is significant because it demonstrates that DTTO fibers have the potential to restore electrical connectivity and facilitate proper cellular communication in excitable cells, which could have important applications in neural and cardiac tissues.

These findings underscore the potential of DTTO fibers as bioelectronic interfaces capable of bridging cellular communication gaps. The ability of these fibers to restore electrical connectivity in cells that have lost their natural gap junctions suggests that they could serve as functional synthetic gap junctions. The potential applications of conductive self-assembled fibers extend beyond the restoration of electrical coupling in isolated cells. In fact, the ability to engineer materials that can seamlessly integrate with biological systems could lead to significant advances in the development of bioelectronic devices that are both functional and compatible with living tissues, paving the way for innovative treatments and therapies.

NOVEL APPROACHES AND MATERIALS FOR HIGH-ORDER HARMONIC GENERATION SPECTROSCOPY

Andrea Annunziata - Supervisor: Davide Faccialà

Since the first observation of high-order harmonic generation (HHG), strong-field physics has rapidly evolved, enabling applications such as the generation of isolated attosecond pulses. These advances have transformed ultrafast science, opening new avenues for time-resolved studies at atomic and molecular scales. Over two decades later, HHG has also been observed in solids, involving electron-hole pair creation, charge acceleration in their respective bands, and recombination, generating harmonics of the fundamental laser frequency. While solid-state HHG has been considered a compact extreme ultraviolet source, it has been primarily valued for its spectroscopic capabilities. More recently, its observation in liquids has expanded the exploration of strong light-matter interactions in this phase.

HHG spectroscopy has enabled the study of various phenomena and the extraction of quantitative material insights. Key applications include all-optical band structure reconstruction and Berry phase characterization. Its success as a spectroscopic tool has driven advancements in time-resolved HHG methods, leveraging its exceptional spatial and temporal resolution.

The harmonic spectrum encodes information about the sample under investigation. Analyzing the polarization state of harmonics helps disentangle different physical processes occurring during strong-field excitation, revealing microscopic mechanisms. Time-resolved HHG measurements further enable the characterization of ultrafast electron and hole dynamics with extreme spatial and temporal resolution. These capabilities can also be extended to liquid crystals, a unique phase of matter where molecules exhibit partial orientational and spatial order, higher than in conventional liquids but lower than in crystalline solids.

In this thesis work, I developed the experimental setups for polarization- and time-resolved HHG experiments in semiconductors and liquid crystals. Figure 1 shows the schematic of the setup for HHG spectroscopy in semiconductors. A 3.2 μm driving field passes through a half-wave plate (HWP) and a linear polarizer (LP1) before being focused by a lens (L1) onto the sample mounted on a rotational stage. The reflected harmonics are collected by a lens (L3) and analyzed using a custom-built polarimeter, consisting of an achromatic quarter-wave plate (QWP) and a linear polarizer (LP3), both mounted on motorized rotational stages. The harmonics are then directed into a visible-ultraviolet spectrometer via an additional lens (L4). This setup allows full characterization of the harmonic polarization state from 1100 nm to 400 nm as a function of the crystal axis orientation.

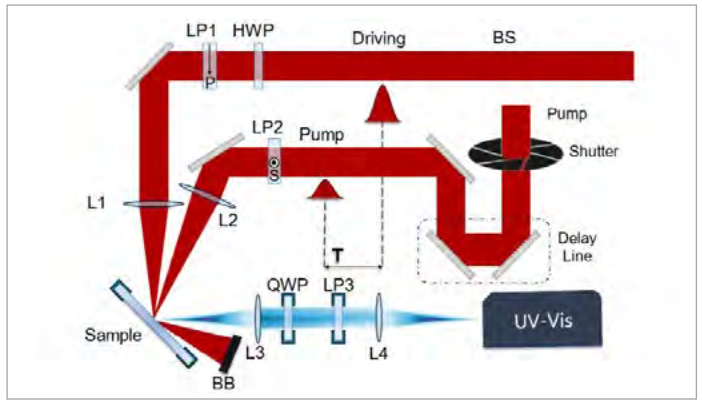

Fig.1 - Experimental setup built for performing polarization and time-resolved HHG experiments in semiconductors.

A second beam, the pump, is directed through a delay line and a linear polarizer (LP2) before being focused by a lens (L2) onto the sample. Pump wavelengths of 3.2 μm, 800 nm, and 400 nm can be selected for time-resolved experiments.

Figure 2 shows the polarization ellipse parameters of the HHG radiation emitted from a Germanium sample as a function of the angle α, which represents the relative orientation between the driving field polarization and the sample. The time-resolved scheme was not used in this experiment.

The intensity of the emitted harmonics varies with α (Fig. 2a), reaching a maximum when the laser polarization aligns with the sample's direction of maximum symmetry. The ellipticity (Fig. 2b), which indicates both the degree of ellipticity of the emitted harmonic, shows a large value for the fifth harmonic at photon energies around 2 eV when the laser field is oriented along a non-symmetry direction of the crystal. It is negative for $\alpha < 45^\circ$ and positive for $\alpha > 45^\circ$. A similar trend is observed in the same energy region for the ellipse orientation β (Fig. 2c), while the regions at $\alpha < 45^\circ$ and $\alpha > 45^\circ$ show opposite helicity.

This energy region corresponds to what is commonly referred to as a Van Hove singularity, a singularity in the electronic density of states that causes an abrupt change in inter-band harmonic emission. The high ellipticity is currently attributed to the emission of different contributions in the harmonic spectrum, each with a distinct polarization state and emission phase. When combined, these contributions produce the complex polarization response observed in Fig. 2. We are currently performing calculations based on the semiconductor Bloch equations to confirm this interpretation.

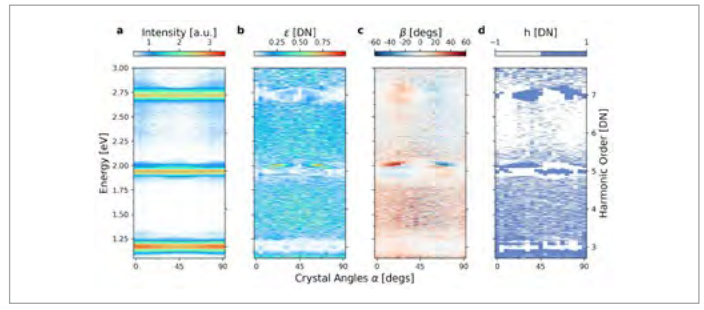

Fig.2 - a) Intensity, b) ellipticity, c) ellipse orientation, d) helicity of the emitted harmonics up to the seventh order.

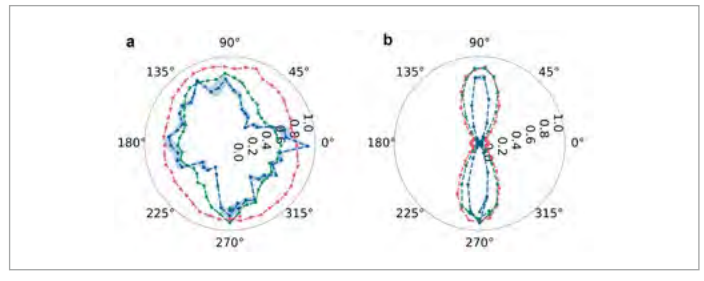

Fig.3 - Harmonic intensity as a function of the laser polarization in the isotropic (a) and nematic (b) phases.

Part of this thesis is also dedicated to HHG in liquid crystals (LCs), an activity conducted at the Max Planck Institute for Nuclear Physics. These experiments involved thermotropic liquid crystals, which exhibit different phases depending on temperature. The primary phases of interest were the isotropic phase, where neither spatial nor orientational order is present, and the nematic phase, where an external voltage induces orientational order in the material. The results obtained for 8CB (4-Octyl-4-biphenylcarbonitrile) are shown in Figure 3. In the isotropic phase, the harmonic intensity varies with the driving field polarization direction. In contrast, the nematic phase exhibits a bilobate distribution, with maximum harmonic emission occurring when the driving field is polarized perpendicular to the axis along which the molecules are aligned. This behavior highlights the strong sensitivity of HHG to the specific phase of the LCs under study.

A NOVEL FOURIER TRANSFORM HYPERSPECTRAL SYSTEM FOR MULTIMODAL WIDE-FIELD RAMAN MICROSCOPY

Benedetto Ardini - Supervisor: Cristian Manzoni
Co-Supervisor: Gianluca Valentini

Hyperspectral Imaging (HSI) is a powerful technique to investigate materials in a non-invasive way by retrieving their spectral signatures. This technology, whose applications span from large Field-of-View (FOV) remote sensing to microscopy, combines an imaging system, which collects a 2D spatial map of the scene, with a spectrometer, which acquires the spectral information of the light emitted, reflected, transmitted or scattered by the objects. The spectrometers used in HSI are of two types: dispersive spectrometers, which spatially separate different wavelengths of light, and Fourier Transform (FT) spectrometers, which capture the light's interferogram and retrieve the corresponding spectrum through the FT operation.
Although FT spectroscopy provides significant advantages over dispersive techniques for HSI applications—such as an improved spectral accuracy, parallel spectra acquisition, shorter measurement times, and flexible interferogram sampling strategies for selecting the relevant spectral features—its use is limited by the inherent instability of interferometers. This limitation restricts the application of FT HSI systems only to the infrared (IR) spectral range, preventing measurements in the visible (VIS) or ultraviolet (UV) ones, unless the setups' complexity is significantly increased. At the same time this drawback limits the maximum achievable spatial resolution of FT systems with respect to the dispersive ones as only longer wavelengths can be exploited.
A prominent field of the HSI is the Raman microscopy which has been adopted in many research fields, such as material science, biology and medicine, due to its high specificity in identifying and classifying the chemical species in the acquired FOV. This technique, which retrieves the vibrational-modes of molecules, typically exploits a point-mapping of the sample with a monochromatic laser in the VIS or near IR spectral range and a dispersive spectrometer to detect the Spontaneous Raman (SR) spectrum of each spatial position in the FOV. However, despite this great potential, Raman microscopy is limited by long measurement times (~10 hours for 10^5 pixels image) and its results are typically hindered by a strong photoluminescence (PL) background, which often overwhelms the amplitude of the Raman peaks.
In this research work a novel Raman hyperspectral microscope (HSM) has been developed that overcomes the typical limitations of Raman microscopy.

This microscope, whose scheme is reported in Figure 1, is based on an innovative birefringent interferometer, the Translating-Wedge-Based Identical Pulses eNcoding System (TWINS), which can allow FT-HSI measurements from the IR to the VIS and UV ranges thanks to its unique long-term stability (better than 1/360 of the optical cycle). The TWINS allows us to retrieve wide-field SR maps with high spatial (~1μm) and spectral (~23cm^{-1}) resolution, high Raman-shift accuracy (<1cm^{-1}) and ~100-times faster measurements (~10 minutes for 10^5 pixels image) than standard Raman systems. Moreover, the FT approach allows us to disentangle SR and PL signals, thus making the Raman HSM a multimodal platform for the detection of separated and sequential maps of these two different optical phenomena in the same sample's FOV.
Figure 2 shows the multimodal measurements of a multi-layer WSe_2 sample illuminated by a uniform 532-nm laser. In this case the PL map gives the relevant information on the spectral heterogeneity of the monolayer region, due to the different strain in different spatial positions; on the other hand, SR provides unambiguous information on the number of layers by detecting a shift of ~3cm^{-1} of the characteristic vibrational peak.

Beside the capability to provide important information for the study of innovative materials, as in the case of WSe_2, the Raman HSM has proven to be a promising setup to be exploited for rapid assessment of microplastics (MPs) pollution. Figure 3 shows the results of a SR measurement (62.5-kpixels image acquired in just 19 minutes) of particles filtered from a seawater sample. The retrieved map allows us to distinguish the calcite ($CaCO_3$), naturally present in the marine environment, from MPs' fragments of PET originated from bottles' wastes. This measurement shows the capability of the HSM to detect the SR peaks from small particles with size lower than 10μm: a limit that other vibrational microscopy systems typically exploited for MPs identification, such as FTIR setups, cannot achieve.

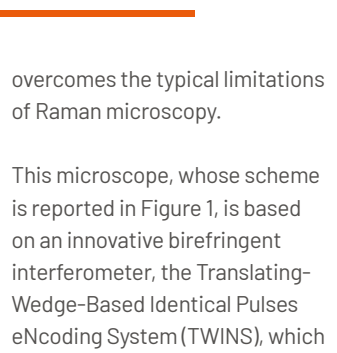

Fig.1 - Schematic representation of the Raman HSM. F: optical multimode fiber. DM: dichroic mirror. TL: tube lens. SPF: short-pass filter. LPF: long-pass filter. RS: Raman signal.

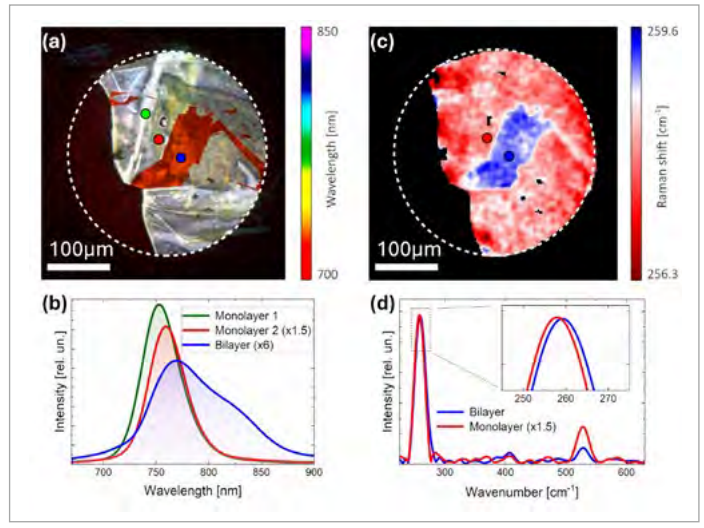

Fig. 2- (a) False colour RGB map retrieved from the PL measurement. (b) Spectra related to the regions outlined by colour circles in panel (a). The scale factors are indicated in the legend. (c) Map of the SR peak detailed in panel (d). (d) SR spectra related to the regions outlined by circles in panel (c). The scale factors are indicated in the legend. The inset shows the detail of the main SR peak.

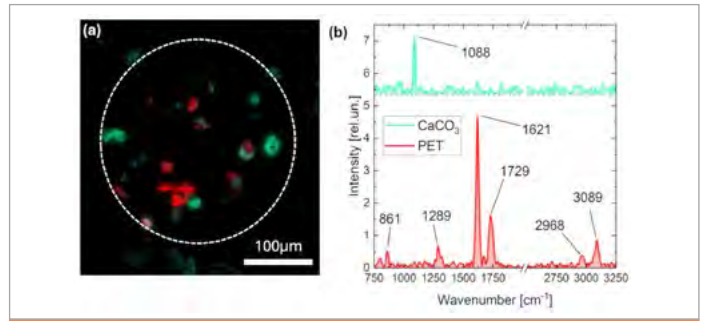

Fig. 3 - SR map of particles filtered from a seawater sample. (a) Composite map of endmember spectra shown in panel (b). (b) Endmember spectra retrieved by N-FINDR analysis distinguishing between PET MPs and $CaCO_3$ grains.

INTERSUBBAND TRANSITIONS IN GE/SIGE QUANTUM WELLS FOR ADVANCED MID-INFRARED INTEGRATED PHOTONICS

Stefano Calcaterra - Supervisor: Jacopo Frigerio

The mid-infrared (MIR) spectral region has recently been subject of important research efforts due to the presence of the *fingerprint* region, where the vibrational frequencies of most molecules lie. A photonic device operating in this region would serve in the detection, identification, and quantification of chemical species, with applications in healthcare, safety and security, and environmental monitoring. Among the several material platforms under investigation, Si-based materials can provide high-density photonic platforms while exploiting state-of-the-art fabrication technologies in a large wafer size. However, typical Si-based choices, such as Si_3N_4 and silicon-on-insulator, are limited to ~5 μm wavelength, due to the strong phonon absorption that occurs in SiO_x. Promising material platform to overcome these limitations are Ge-on-Si and SiGe-on-Si: the wide Ge transparency window makes it possible to work in the full MIR spectral range (3-15 μm).
A possible implementation of several photonic building blocks is the exploitation of intersubband transitions (ISBTs) in Ge/SiGe multiple quantum wells (MQWs), e.g. in a quantum well infrared photodetector (QWIP).
I n the first part of the work, a MQW heterostructure was designed, by the Luttinger-Kohn model implemented in commercial software *Nextnano*, to confine two heavy-hole levels with an energy spacing ~150 meV, thus featuring a TM-polarized ISBT around 8.3 μm.
The structure was then epitaxially grown by low-energy plasma-enhanced chemical vapor deposition (LEPECVD) in the L-NESS facility. A specific growth protocol had to be developed to achieve high compositional mismatches in few nanometer thick layers.
The optimization of the growth process has been supported by an extensive structural characterization, by means of high-resolution X-ray diffraction and atom probe tomography.
In order to induce ISBTs-related absorption a normal incidence geometry cannot be adopted, because of the polarization selection rules governing such optical transitions. For this reason, prism waveguides were fabricated (Figure 2a).
Temperature-dependent dichroic transmission spectra were measured using a Fourier-transform spectrometer (FTIR). The spectra presented, at 10K, a ~25meV large dip at 145 meV (~8.5 μm) associated with ISBT absorption (Figure 1b).
The complex evolution of the spectra with temperature was interpreted with the support of a refined tight-binding.
The second part of the work, mainly carried out at C2N – Universitè Paris-Saclay under the supervision of Prof. Delphine Marris-Morini, regarded the design, fabrication and electro-optical characterization of a room-temperature waveguide-integrated QWIP.
The design process, based on Ansys Lumerical MODE simulations, regarded the engineering of the refractive index profile and of the metallic contacts shape (Figure 3a) to allow the existence of a propagating TM mode in the device, while ensuring a significant overlap with the active region.
The devices were then fabricated and characterized at room-T: responsivity spectra presented peaks in the 7-9 μm range under TM illumination, while TE illumination provided rather flat spectra (Figure 3b). The external responsivity was measured, with a value of 1.8 mA/W at 7.8 μm.
In conclusion, realization of a MQW platform featuring an ISBT in the MIR spectral range has been achieved, along with a growth protocol which enabled the realization of more complex well shapes. A proof-of-concept waveguide-integrated QWIP operating at room temperature has been demonstrated, with promising results towards the integration of a group-IV QWIP in a PIC.

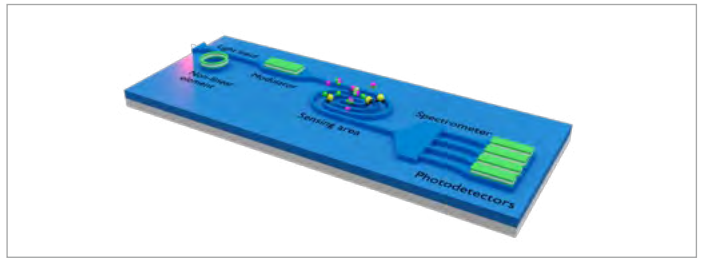

Fig.1 - Sketch of a photonic integrated circuit for sensing purposes. In green some building blocks which can be realized leveraging on ISBTs in Ge/SiGe QWs are highlighted.

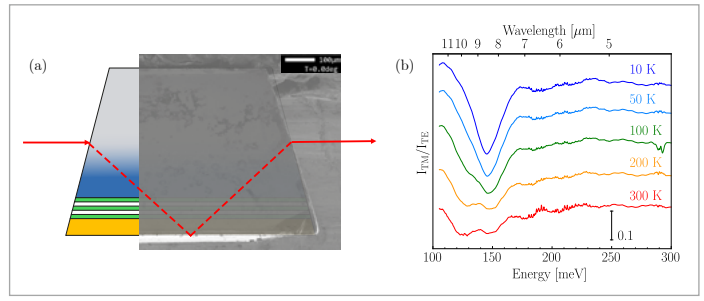

Fig.2 - Sketch of the light path in a prism waveguide. A SEM image of the prism is superimposed. (b) Temperature-dependent dichroic absorption spectra of one sample. The sharp ISBT absorption dip at 10K evolves into a double larger dip at room T.

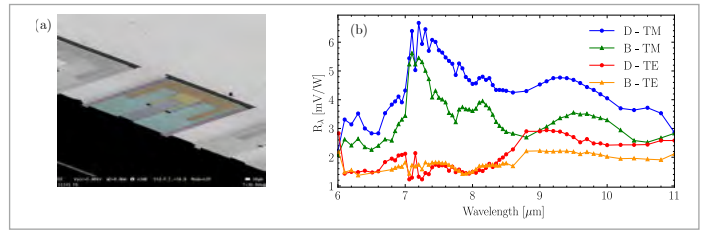

Fig.3 - (a) SEM image of the fabricated device: in yellow and orange the gold pads, in blue the mesa and in purple the trench to define the waveguide. (b) Relative responsivity spectra under TM (blue and green) and TE (red and orange) polarized illumination.

FOOD-BASED PRINTED INTEGRATED LOGIC CIRCUITS

Giulia Coco - Supervisor: Mario Caironi

The growing interest in ingestible devices that enable personalized medicine creates an urgent need to develop solutions using safe and sustainable materials. This approach aims to facilitate broader integration of the technology into everyday healthcare applications. While the concept of ingestible electronics is indeed fascinating, numerous challenges remain, primarily concerning the risks associated with non-degradable materials, which pose issues related to their retention in the gastrointestinal tract. Furthermore, these devices, which are designed to be disposable, depend on CMOS chips for computation and control, resulting in resource waste and significantly impacting the environment by contributing to the generation of E-waste. In this context, edible electronics is emerging as an innovative field to address and overcome these limitations. By leveraging the electronic properties of food additives and derivatives, it seeks to realize safe-to-eat devices that seamlessly integrate with biological systems. Such devices alleviate concerns regarding toxicity and environmental impact, making them ideal candidates for applications in personalized medicine, diagnostics, and even smart food packaging. Looking ahead, edible electronic circuits could be combined with edible sensors, actuators, and energy sources to create robotic food or edible robots. Their applications could range across various domains: for instance, edible robots might mimic prey to attract wild animals for vaccine administration, or robotic food could offer novel culinary experiences. These robots could either perform their functions outside the body, then be safely eaten and eventually metabolized, or be designed to operate within the body before being processed by the GI tract. Transistors fabricated using almost only edible materials have been reported, and, in some cases, their use in circuits has been investigated. However, there is a lack of systematic work on the fabrication and characterization of edible integrated logic circuits. The main focus of this dissertation is the fabrication of integrated logic circuits using food additives and derivatives, with inkjet printing as the main deposition technique. These circuits will provide computational and control functionalities for future edible systems. The research activities of this thesis involved the choice of materials, the formulation of printable inks, the optimization of the design and fabrication, and the electrical characterization of the final devices. A flexible and water-insoluble ethyl cellulose film was selected as a substrate for all the fabricated devices, as this would allow them to be conformable with various edible systems, for example, pharmaceutical capsules (Figure 1). At first, the design and fabrication of a fully printed potentially edible transistor were optimized for operation at low voltage (0.7 V) and for low leakage. The operation at low voltage was possible using electrolyte-gated transistors. Chitosan, derived from shrimp and crab shells, was selected as the material for the electrolyte. A coplanar gate was designed to favor the integration in complex circuits by having all the electrodes on the same level. The reduced leakage was obtained thanks to the formulation of an edible inkjet-printable passivation layer, lacking in the current state of the art, based on shellac, a naturally occurring resin. Inkjet printing was chosen as a deposition technique because it is additive, scalable, and requires low temperatures. A benchmark p-type biocompatible semiconductor was selected, and preliminary toxicity tests were conducted upon simulated digestion of the device, revealing no adverse effects on the intestinal cells and suggesting the potential edibility of the fabricated transistor. All the used food additives are present in quantities well within the accepted daily intake defined by the European and American food safety authorities (EFSA and FDA). The next step involved the design, fabrication, and characterization of an edible resistive load to implement in a unipolar configuration with the fabricated transistor. A fully printed resistor that allows the realization of integrated logic circuits was inkjet-printed using the same materials used for the fabrication of the transistor. Four unipolar integrated logic circuits were implemented and demonstrated, namely NOT gate, NAND gate, SR latch, and a three-stage ring oscillator, all operating at 0.7 V, which is a voltage compatible with safe contact with the human body. While these results are cutting-edge, unipolar logic has inherent limitations that could be addressed by transitioning to a complementary configuration, which is the most commonly used in modern electronics for its great efficiency. The last part of this work describes the realization of edible complementary logic circuits starting from fully edible transistors exploiting two types of copper phthalocyanines, used as cosmetic pigments and present in commercial toothpaste, as p- and n-type semiconductors. Besides the semiconductor, these transistors exploited the same materials found in the transistors employed in the unipolar configuration. The chosen structure is the top gate bottom contacts. Complementary integrated edible logic gates and circuits operating at voltages between 0.5 V and 1 V were demonstrated, namely a NOT gate, NAND gate, and a three-stage ring oscillator. Stability of over 2 months was assessed. All the fabricated logic circuits were integrated with an edible energy source, specifically an edible rechargeable battery with a capacity of up to 20 µAh and a voltage of ~ 0.7 V (Figure 2). The successful demonstration of their compatibility proves that powered edible logic circuits are possible. The development of edible electronics represents a groundbreaking frontier in technology. Even though many challenges still need to be overcome to integrate it into real applications, this work lays the foundation for future advancements and paves the way for solutions in healthcare, food monitoring, and edible robotics.

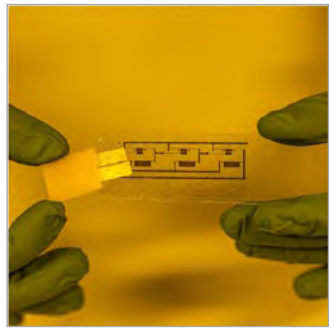

Fig.1 - Fully printed edible electronic circuits on flexible ethyl cellulose substrate rolled inside pharmaceutical capsules.

Fig.2 - Demonstrative picture of the connection between a fully printed edible logic circuit and an edible rechargeable battery.

BENCHMARKING QUANTUM MACHINE LEARNING FOR QUANTUM CYBERSECURITY

Sebastiano Corli – Supervisor: Enrico Prati

Quantum computing is envisaged as a revolution in many fields of computer science. Its promising applications range from cryptography to logistics, optimization, molecular dynamics, machine learning and cybersecurity. The first insight of a quantum supremacy of quantum computation over its classical counterpart arose in 1994, when Peter Shor designed a quantum algorithm capable to find the prime factors of any integer number in a polynomial time. The same problem, nonetheless, on a classical device scales with an exponential trend by adding more digits on the integer to be factorized. A specific field of research thus inquires about possible advantages of employing quantum algorithms in computer science. In the domain of cybersecurity, many classical techniques of machine learning have been tested, some of which nevertheless prove to scale as NP-hard by increasing the size of the system.

Leonardo S.p.A. has funded this PhD scholarship in order to explore new potential benefits from quantum computing, which more specifically addresses the research area of machine learning. The interests of the company range from quantum communication, in order to enhance quantum-based solutions applied to communication systems to increase their security, to quantum sensing for optronic systems and radio frequency sensors. In the AI field, quantum computing is being explored to leverage algorithms that are designed to reduce the complexity of NP-hard problems, with a specific focus on cybersecurity. One specific area of cybersecurity where quantum computing is proving promising concerns graph problems and data clustering. Clustering algorithms, indeed, can be addressed to perform network traffic identification on graph-based network security. When characterizing the network traffic, a novel approach consists of representing the servers as nodes of a graph, and the flow of data between them as the edges of the graph itself. By monitoring the topology of the graph, relying on a technique called graph similarity, any anomaly can be straightforwardly detected. Nevertheless, despite the effectiveness of such approach, the graph encoding for anomaly detection turns the problem to an NP-hard one by scaling with the number of nodes. Instead, quantum computation is able to tackle graph-based problems in a polynomial time.

Despite the great promises and hype behind quantum computing, nowadays many hurdles still prevent us to employ fault-tolerant quantum machines in everyday tasks. Still, many technologies, e.g. trapped ions, superconducting qubits, or neutral atoms, are in contention for the development of robust and noiseless devices. Among these competitors, photonics plays a major role, due to its range of applications and its overlap with quantum communications. Manipulating single photons provides to set digital computing with discrete variables (qubits) to analog computing on continuous variables (qumodes). Moreover, switching from general-purpose to purpose-oriented quantum computing, Gaussian boson sampling allows to perform tasks which are NP-hard on classical devices.

In order to improve the robustness of the quantum devices, algorithms need to be taylor-suited for specific devices, in order to reduce the amount of hardware resources required for the computation. Apart from improvements in the field of error correction and mitigation, such reduction task can be performed in the field of quantum compiling, i.e. studying opportune techniques to compose unitary operations between the qubits, tackling the implementation of specific algorithms and routines on a quantum computer. In the field of quantum compiling, one of the paramount aims consists of reducing the number of required ancillary qubits when implementing quantum circuits. In linear optics, due to the lack of interaction and therefore of entanglement between photons, the textbook architecture of compilation is measurement-based quantum computing. Within this frame, quantum measurements are employed to make superposition states collapse and therefore implementing two-qubits (or even more) logic operations. Nevertheless, such paradigm of computation can be further extended even to non-photonic hardware, on which deterministic entangling operations are available.

In this Thesis, we focus on a notorious algorithm in literature, the QAOA, a practical example of quantum machine learning in the NISQ era. The QAOA is widely envisaged in literature as an algorithm oriented to solve graph-based applications, many of which are already employed for cybersecurity tasks. To assess the potential of QAOA on photonic platforms, we run this Thesis on the following scheme. The first Chapter details the groundings of quantum optics oriented to photonic computing, introducing furthermore the principles of measurement-based quantum computing. The second chapter focuses on the graph states, their algebraic description, and the topological properties of the stabilizers. Furthermore, a novel formalism to describe the graph states, which reduces the number of stabilizers to fix their topology, is introduced.

The third Chapter introduces new compiling techniques we develop to suit one-way quantum computers. Instead of translating the gate model circuits into a graph state, this new method tightens the measurement-based compiling to a native method which does not involve any transpiling from the gate model. Eventually, a gauge theory for mapping unitary operators into graphs emerges, allowing multiple graph states to implement a given unitary operation. Due to this additional degree of freedom, an efficient compiling can be achieved by adapting the most suitable gauge for the algorithm to be compiled. The fourth Chapter selects the QAOA as a candidate algorithm for benchmarking the complexity of operations between the gate model and in the measurement-based paradigms. Comparing these two architectures of computation, we try to select which of them is the most promising candidate for a direct implementation on cybersecurity tasks. Such benchmark has been settled both on a theoretical framework and a classical HPC emulation of the algorithm under investigation. At the very beginning of the Chapter, the groundings of the QAOA are settled, deducing its formulation from the adiabatic theorem.

DEVELOPMENT AND CHARACTERIZATION OF A FOURIER-TRANSFORM HYPERSPECTRAL CAMERA IN THE THERMAL INFRARED BASED ON A BIREFRINGENT INTERFEROMETER

Matteo Corti - Supervisor: Gianluca Valentini

Hyperspectral imaging (HSI) combines the spatial information provided by imaging techniques with spectral knowledge, allowing one to obtain a full spectrum for each pixel of a bi-dimensional detector. The obtained three-dimensional datum is called spectral hypercube and can be seen as a stack of images taken at different wavelengths. The technique can either be performed in the spectral domain or in the time domain. In the first case, a series of bandpass filters are placed in front of the imaging optics, each enabling the acquisition of an image in a narrow spectral band. Alternatively, a combination of a slit and a dispersive element, such as a prism or a grating, can be used to acquire the spectrum in each point of the field of view with a line-scanning acquisition. In both cases, the spectral or spatial filtering operation blocks much of the light. The time domain approach exploits instead the principle of Fourier-transform (FT) spectroscopy: the impinging light is separated by an interferometer in two delayed replicas, which then interfere in each pixel of the sensor. Scanning the relative delay makes it possible to acquire a series of images in different interference conditions so that each pixel measures an interferogram. This can be converted into the corresponding spectrum by performing an FT operation. The approach has a throughput advantage compared to spectral domain acquisition since no filtering operation is performed, and also a signal-to-noise advantage, considering equal throughput and spectral resolution. These benefits turn especially useful in the thermal infrared (TIR) spectral region, with wavelengths from 3 to 14 μm. In fact, the small bandgap of quantum sensors for this range makes cryo-cooling necessary to prevent thermal excitation of carriers, determining bulky and expensive systems. Thanks to the higher signal, FT HSI enables the use of thermal sensors like microbolometers as an alternative, which are not usually coupled to spectral-approach instruments due to their low sensitivity. Nevertheless, they have good spatial resolution and require no cooling systems, giving a huge advantage in size, weight, and power (SWaP). In the work presented here, a microbolometer thermal camera with 640×480 pixels was coupled to an innovative birefringent interferometer, the Translating-Wedge-based Identical pulses eNcoding System (TWINS). In this device, the impinging light is separated in orthogonally polarized replicas by a 45-degree polarizer. The delay is achieved by the use of two birefringent crystals with orthogonal axes, the second of which is divided into two wedges that can relatively translate along the hypotenuse by using a motorized stage. This allows control of the overall optical thickness and therefore of the delay between the replicas, which then can interfere after a second 45-degrees polarizer that projects the replicas' electric fields along the same axis. Compared to the classical Michelson interferometer, TWINS is more compact and stable, since mechanical vibrations are rejected by the common-path scheme. The most suited crystal for TIR is Hg_2Cl_2, known as calomel. Its high birefringence determines however a large lateral walk-off between the two replicas, strongly reducing the interferometric contrast. To compensate for this, a new design was devised and implemented. The interferometer was calibrated with the use of quantum cascade lasers and a single-pixel mercury-cadmium-telluride detector. It was then tested by measuring the spectrum of coherent pulses with band extending from 8 to 11 μm and produced by difference-frequency generation (DFG) in a nonlinear crystal from an input Er laser. Fig. 1 (a) represents the interferograms of the raw pulses and the same after propagation through a bandpass filter centred at 9 μm. An interferometric contrast of 98% was achieved. Fig. 1 (b) shows the corresponding spectra and a comparison with measurements from a commercial FTIR instrument. The maximum achievable spectral resolution is 4.25 cm^{-1}. After successful tests with incoherent radiation, the hyperspectral instrument was built by placing TWINS in front of the microbolometer thermal camera, equipped with a 35 mm objective. The instrument weighs about 1 kg, has a volume occupation of 15×30×10 cm^3, and a power consumption of a few watts, determining a large SWaP improvement compared to current HSI systems in the infrared. Imaging capabilities were tested both in transmission and emission geometry. In the former case, different plastic films in front of a hotplate at 650 K, used as a source of thermal light, were successfully distinguished through their infrared absorption peaks, thanks to their distinctive vibrational levels. In the latter case, a quartz crystal and a 1-inch fused silica window were placed on top of the same hotplate. In this situation, the objects themselves were the sources of radiation. Fig. 2 (a) shows a false-color image of the scene generated from the spectral hypercube. Fig. 2 (b) displays the spectra of the corresponding numbered regions. The good spatial contrast of the image can be attributed to the rich spectral information present in the scene. In particular, spectra 1 and 4 differentiate crystalline and amorphous quartz, due to a Reststrahlen band strongly decreasing the emissivity in the crystalline form. These chemometric capabilities, together with the system's compactness, make it ideal for on-site remote sensing applications.

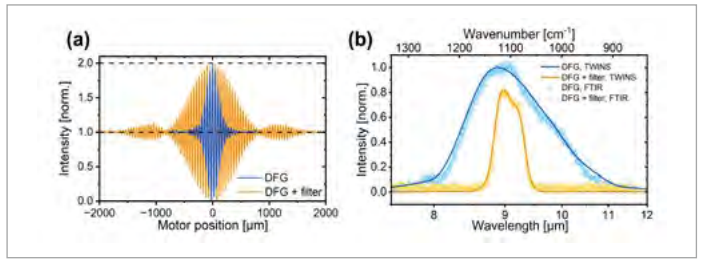

Fig.1 - (a) Interferograms of the bare DFG light (blue) and of the same light after propagation through a bandpass filter centred at 9 μm (orange). (b) Spectra retrieved as FT of the same-colour interferograms (solid lines) and measured by a commercial FTIR instrument (circles).

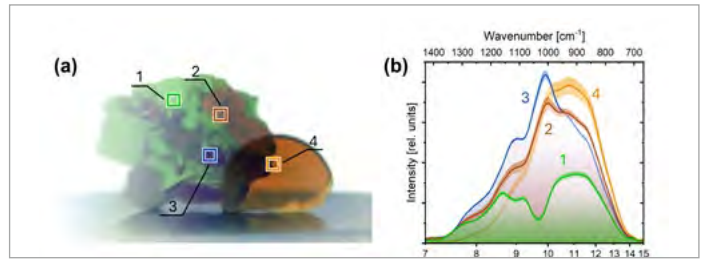

Fig.2 - (a) False-color image synthesized from the spectral hypercube of a quartz crystal and a 1-inch fused silica broken window on top of a hotplate at 650 K acquired with the hyperspectral camera. (b) Emission spectra with error bars corresponding to the numbered regions.

SPIN COMPUTING

Andrea Del Giacco – Supervisor: Federico Maspero

Spin computing, which harnesses the spin state in magnetic materials to process information, has emerged as an alternative to traditional electronics. Specifically, we focus our attention on Magnonics, the study of the excitation of the spin lattice in magnetic materials, known as spin waves (SW). They offer non-volatility, a non-linear dispersion relation, and high-speed operation. The more, their intrinsic nature allows operation in the radio frequency (RF) regime with spatial wavelengths ranging from a few micrometers to nanometers, demonstrating the feasibility of spin-integrated RF components. However, translating SW concepts into practical devices faces two major challenges: integration with existing electronics and material limitations. Achieving controlled SW propagation in advanced architectures requires materials with tailored magnetic anisotropy and minimal defects, necessitating innovative solutions for their fabrication and tunability. The most suitable material choice is the family of rare-earth iron garnets (REIG). This class of materials exhibits extremely low damping and offers the unique ability to tune the magnetic anisotropy landscape. Among these materials, Yttrium Iron Garnet (YIG) has demonstrated the lowest damping retrieved so far. Nevertheless, they can only be properly grown on gadolinium gallium garnet (GGG), limiting their integration. Furthermore, their magnetic properties are extremely sensitive to any machining of the samples. To address these challenges and demonstrate the potential of this technology, we investigated laser patterning and YIG-MEMS integration as strategies to overcome both fabrication and integration limitations. Additionally, using the micromagnetic simulation environment Ubermag, we developed a simulation system to test the feasibility of innovative devices and fine-tune their fabrication constraints. The main part of these activities was carried out at Polifab, the micro- and nanofabrication center of Politecnico di Milano. Laser patterning was performed with a soft UV laser (405 nm) on amorphous, non-magnetic REIG to induce local crystallization of the sample. This exploits the fact that the magnetic signature is strongly related to the crystallinity of the specimen. Such a system enables the direct writing of magnonic circuits embedded in non-magnetic matrices, where spin excitations are inherently confined in the patterned racetracks. We were able to obtain a magnetic damping one order of magnitude worse than state-of-the-art YIG films, and to propagate SW over tens of μm. We are now also investigating Bi-doped YIG films, where it is possible not only to induce magnetic racetracks but also to tailor the magnetic anisotropy according to the laser fluence, paving the way to the realization of complex magnetic landscape at the micro-scale. This technique not only allows arbitrary shape patterning but also prevents physical machining of the sample, avoiding physical or chemical etching. However, to ensure proper crystallization, a suitable lattice match with the substrate is necessary, achievable only among garnets. To overcome the integration constraint, we explored the integration of YIG with MEMS technology within the European consortium MandMEMS (project number 101070536), providing a pathway to hybrid systems that bridge spin devices with silicon electronics. Such integration not only exploits state-of-the-art YIG films but also allows tuning the propagating waves based on the MEMS' relative positions. We demonstrated the functionalization of MEMS with magnetic materials—Permalloy (Ni20Fe80)—and coupled this system with magnonic platforms. In figure 1, we illustrate a hybrid system capable of modifying the magnetic landscape of the magnonic component based on MEMS actuation. A spin wave is injected and detected in an 800 nm YIG film using radiofrequency transducers. Depending on the relative position of the Ni20Fe80 micromagnet, it is possible to tune the frequency bandwidth of the device, paving the way for RF computing elements. Our first proof of concept demonstrated the realization of a delay line where the SW pocket is shifted in frequency according to the DC voltage applied to drive the MEMS and the external magnetic field. Recently, we also focused on the possibility of modulating spin waves by engineering the global magnetic landscape of a system. Specifically, our attention was directed toward magnetic/non-magnetic multilayers, investigating the feasibility of computational tasks in vertically coupled magnonic waveguides. We designed a system based on dynamic dipolar interactions between two magnetic layers separated by a non-magnetic spacer. In figure 2, we report the spin wave dispersion relation of such a system. By locking at a precise frequency, two different wavelengths can be excited, opening possibilities for multiplexing and demultiplexing tasks, relying on a frequency-dependent interference pattern that can be established in the system. A deep simulation optimization was carried out for two different systems: CoFeB/MgO/CoFeB and YIG/GGG/YIG heterostructures. We investigated how geometrical and magnetic parameters impact the dispersion relation and the coupling response of the system. Recently, preliminary test devices have been fabricated and are currently under investigation.

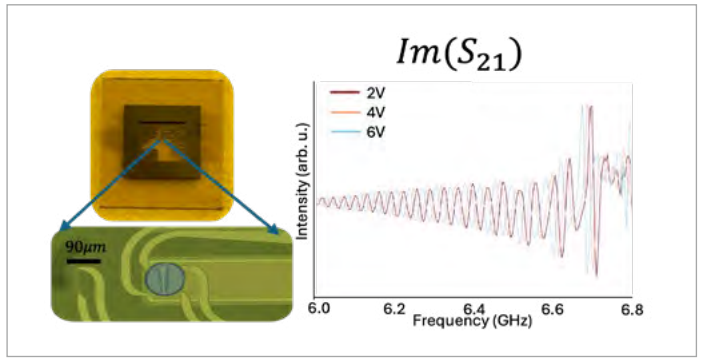

Fig.1 - Optical images of the magnonic-MEMS hybrid system (left). Frequency shift as a function of the MEMS applied voltage (right), measured under a magnetic field of 160 mT.

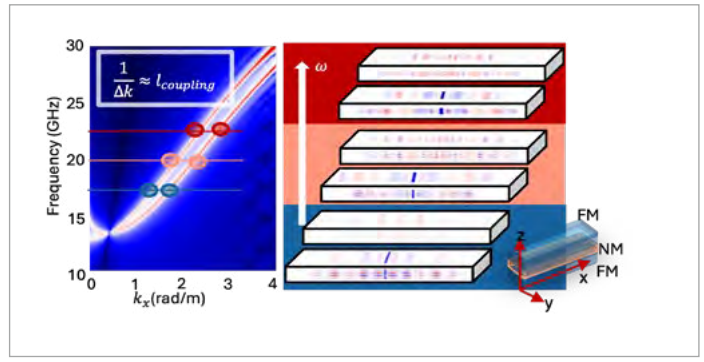

Fig.2 - Micromagnetic simulation of the band dispersion (left) and the associated spatial interference (right), illustrating the frequency dependence of the spatial modulation (i.e., the coupling length).

MODULATION AND ROUTING OF NONLINEAR OPTICAL SIGNALS AT THE NANOSCALE

Agostino Di Francescantonio - Supervisor: Michele Celebrano

Nanophotonics is a growing research field, aimed at developing miniaturized photonic devices for light manipulation in a sub-micrometer thickness.
A precise control of the light properties in ultrathin platforms can unlock applications ranging from the realization of flat optical elements to optical computing, light detection and ranging (LiDar) and sensing. The challenge in downscaling photonic processes, in particular nonlinear ones, resides in the weak interaction strength of photons with matter, requiring a propagation length inside a material of the order of the millimeter. While this fundamental limitation can be surpassed on-chip by confining light in photonic waveguides, it restricted the manipulation of freely propagating beams to bulky refractive or diffractive optical elements.
Inspired by R. P Feynman celebrated talk "There's plenty of rooms at the bottom", the manipulation of photons on a small scale can benefit from unique phenomena arising when light interacts with nanostructured materials, nowadays available thanks to the outstanding advancement in nanofabrication technology. Electromagnetic resonances at optical wavelengths occurring when nanostructuring materials, like noble metals and high-refractive index dielectrics, enhance light-matter interaction through field confinement. Moreover, the arrangement of such systems in artificial lattices, i.e. metasurfaces, allows manipulation of the light by for example tailoring the phase profile. Eventually, the meta-atoms collective behavior can result in delocalized resonances, with improved field confinement with respect to the ones occurring in single resonators. Resonances occurring at the nanoscale are also beneficial to downscale nonlinear optical phenomena. Arising in matter when the light intensity is high enough to produce sizable multiphoton interaction, they already found a number of applications, like the generation of ultrashort pulses, the study of surface properties and the generation of entangled photons. The perturbative nature of nonlinear optical interactions limited their use to bulk media, under very precise configurations dictated by the phase-matching condition. While such condition cannot be met at the nanoscale, the field enhancements in optical nanoresonators can alleviate such limitation thanks to the nonlinear dependence of most these processes on the pump light intensity. Moreover, the coherence of parametric nonlinearities, combined with the arbitrary phase introduced by metasurfaces, further enlarges the functionalities attained at the nanoscale in the linear regime.
My PhD activity revolved around the investigation of two nonlinear metasurfaces, leveraging the aforementioned considerations to steer and modulate nonlinear signals.
First, the coherence between nonlinear optical processes was exploited into a ω+2ω double-pumping scheme, developing an interferometric control of radiation at 3ω. A fundamental beam with angular frequency ω in the telecommunication band (λ = 1550 nm) and its second-harmonic (2ω) replica pumped

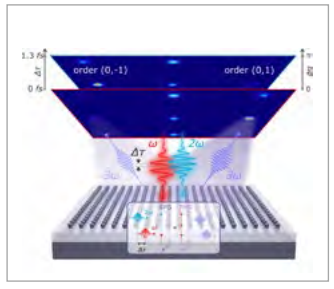

Fig.1 - Coherent routing of a signal at 3ω stemming from nonlinear upconversion of a pulse at ω and its delayed replica at 2ω in a diffractive AlGaAs metasurface. The power at 3ω is routed between (0,±1) orders by applying a delay variation Δτ = 1.33 fs.

third-harmonic generation (THG, ω+ω+ω = 3ω) and sum-frequency generation (SFG, ω+2ω = 3ω). Their far field superposition was controlled adjusting the relative phase between the input beams. The even (odd) number of photons involved in SFG (THG) imply selection rules that quench interference in presence of axially symmetric systems. This causes SFG (THG) to be even (odd) under π rotations, with a total output at 3ω independent on the input relative delay. This argument was demonstrated in AlGaAs single pillars, whose C_4 symmetry hindered interference detection. An effective coherent control requires systems with broken axial symmetry, introduced for example by arranging the cylinders into a diffractive metasurface (see Fig. 1). The steering of the 3ω signal in off-axis directions enabled interference within the individual diffraction orders. Importantly, the opposite parity of THG and SFG was the key to attain the so-called coherent routing of the 3ω radiation, since the fringes of mirror-symmetric diffraction orders resulted in antiphase, with 1.33 fs of switching delay.
Through careful optimization of input powers, laser polarization and lattice pitch, a maximum interference visibility of 90% was achieved.
Nonlinear processes also include electro-optic (EO) effects, stemming from the interaction between optical and static fields. They are exploited to modify material refractive index and reconfigure the optical response of nano-optical devices. In the second part of my thesis, the reflectivity and the second-harmonic generation (SHG) were modulated by means of (EO) effect in a lithium niobate ($LiNbO_3$) metasurface. Spectrally sharp resonances obtained through translational symmetry breaking (see Fig. 2a and b) were exploited to enhance the sensitivity on the refractive index change, obtaining a sizable modulation of both reflectivity and SHG by driving the metasurface with CMOS-compatible biases (see Fig. 2b, c). The SHG background-free character and square dependence on the pump field were pivotal to gain one order of magnitude of SHG modulation with respect to the linear case. Eventually the low capacitance of the device allowed for a bandwidth reaching the GHz range (see Fig. 2d).
My thesis highlights the potential of nonlinear optics at the nanoscale, focusing on the coherence of parametric processes and the nonlinearity itself. The former enables field multiplication, at the basis of phase-sensitive applications controlled by the symmetry of the system. The latter produces an increased sensitivity to changes in the metasurfaces optical properties. The combination of these features paves the way for the development of nanoscale photonic devices extending the functionalities attained in the linear regime.

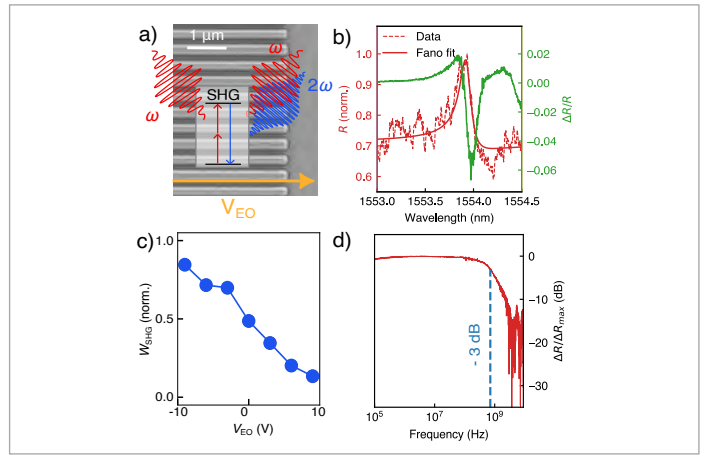

Fig.2 - a) SEM of an asymmetric LiNbO3 grating mediating SHG, biased by an applied voltage VEO. b) Reflectivity (red) and its relative modulation amplitude (green) upon sinusoidal drive with amplitude 10 V and frequency 100 kHz. c) Frequency response of the reflectivity modulation. The blue dashed line sets the -3 dB attenuation. d) Variation of the SHG, excited at 1553.82 nm, depending on the applied voltage.

PHASE TRANSITIONS, DYNAMICS, AND AVALANCHES IN DISORDERED ISING MODELS

Federico Ettori - Supervisor: Paolo Biscari

Modelling complex systems is essential for understanding the emergent behaviour observed in both nature and technology. Phenomena ranging from phase transitions in materials to collective dynamics in biological networks demonstrate how simple interactions can lead to complex, interconnected outcomes. Under the supervision of Prof. Paolo Biscari, I focused my research on the impact of structural disorder on the two-dimensional Ising model by incorporating frozen spins to simulate defects. Using Monte Carlo simulations, I investigated both equilibrium properties and dynamical processes, such as magnetisation reversal and avalanche events. The insights gained inform the design of magnetic storage devices, optimise ferromagnetic thin films, and shed light on earthquake dynamics in geophysics, where similar power-law behaviours emerge.

A novel variant of the classical Ising model was considered, implementing fixed defects by freezing a fraction of the spins. This diluted model creates a complex energy landscape that mimics magnetic impurities in real disordered materials. It shares key features with the Random Field Ising Model while permitting the use of more efficient algorithms. Its innovative design offers fresh insights into altered phase transitions, nucleation phenomena, and avalanche dynamics—a breakthrough that has not been studied before. To probe these effects, two complementary Monte Carlo methods were employed. The N-Fold Way algorithm was used for low-temperature, out-of-equilibrium simulations to efficiently sample rare nucleation events essential for understanding magnetisation reversal. Meanwhile, the Metropolis algorithm with multi-spin coding investigated equilibrium properties by leveraging parallel processing to simulate multiple configurations simultaneously. These methods provide a robust framework for exploring static and dynamic behaviours in disordered magnetic systems.

We initially explored the equilibrium properties of the two-dimensional Ising model with defects. At low temperatures, fixed impurities prevent the emergence of global order, echoing behaviours observed in the Random Field Ising Model. As illustrated in Figure 1, the average spin direction reveals distinct clusters: regions where spins are predominantly positive coexist with areas that are largely negative. These localized microdomains indicate that, while overall magnetisation remains absent, defects induce a non-uniform ordering that disrupts long-range coherence. Furthermore, our analysis uncovers several key findings. Investigations based on the overlap probability distribution reveal a quasi-ferromagnetic phase in small systems with a low fraction of defects, where local ordering becomes prominent. Moreover, the transition from a paramagnetic to a clustered phase is characterised using a novel order parameter since conventional magnetisation fails to capture the change (remaining zero in both regimes). These results provide a detailed picture of equilibrium behaviour in disordered systems and establish a solid basis for subsequent studies on dynamic and out-of-equilibrium properties.

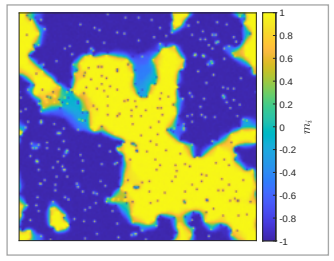

Fig.1 - Equilibrium configurations at low temperature for the two-dimensional Ising model with defects showing the formation of defect-induced clusters at low temperatures, contrasting with the homogeneous Ising model.

We investigated how defects modify the magnetisation reversal process, with a particular focus on re-adapting Classical Nucleation Theory (CNT) for heterogeneous systems. In our model, fixed impurities lower the free energy barrier for forming critical droplets, thereby reducing the critical cluster size required for reversal. As demonstrated in Figure 2, the free energy profile as a function of cluster size (obtained via an Umbrella Sampling procedure) shows remarkable agreement with the CNT-estimated free energy expression. The inset of Figure 2 highlights the reduction effect on the free energy barrier induced by defects. Our CNT analysis allows us to extract the surface tension, which is greatly reduced by the presence of impurities. Furthermore, a detailed analysis of cluster growth velocities reveals that temperature-dependent pinning effects disrupt standard droplet expansion dynamics. The presence of defects accelerates the reversal process, making it more deterministic than in homogeneous systems. These findings validate the re-adapted CNT framework for disordered systems and offer crucial insights into how defects control dynamic switching in real magnetic materials.

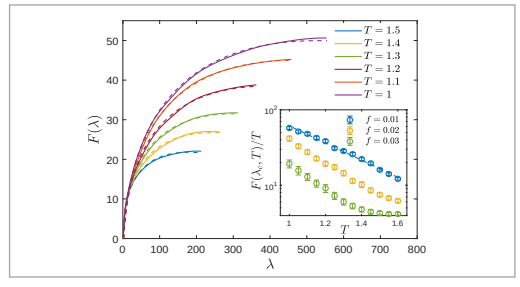

Fig.2 - Free energy landscape as a function of cluster size for the model with defects obtained through direct estimation (solid lines) and classical nucleation theory (dashed lines). The inset shows the free energy barrier as a function of temperature for different defect fractions.

Building on these dynamic insights, we analysed avalanche phenomena and inter-event time (IET) statistics in the Ising model with defects. Focusing on the avalanche size distributions during hysteresis cycles, we found that magnetisation jumps follow a robust power-law behaviour. As shown in Figure 3, the probability distribution of these jumps aligns well with a power-law model, signifying scale-invariant, critical dynamics. The presence of defects not only alters the scaling exponents but also renders the avalanche distributions largely temperature-independent, underscoring the universal aspects of disorder-induced criticality. Furthermore, our analysis of IET statistics reveals stark differences between homogeneous and heterogeneous systems. In a defect-free environment, the IET distribution is typically exponential (Poissonian), reflecting uncorrelated, random events; however, the introduction of defects creates a complex scenario in which the IET distribution transitions to a fat-tailed, power-law form. This shift indicates the emergence of long-range correlations and collective dynamics, emphasizing the critical role that quenched disorder plays in shaping the system's overall response to external stimuli.

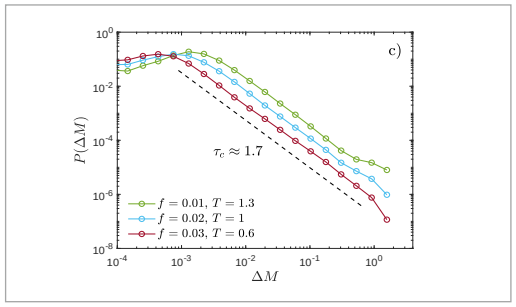

Fig.3 - Avalanche probability distributions demonstrating power-law behaviour at criticality, with a universal exponent $\tau_c \approx 1.7$, independent of temperature.

Ultimately, my work reveals the critical role of quenched disorder in driving nucleation and avalanche processes within the Ising model. This deeper understanding not only enriches our theoretical framework for disordered magnetic systems but also paves the way for practical innovations in the design of advanced materials and devices.

EDIBLE SEMICONDUCTORS: FROM FUNDAMENTALS TO EDIBLE LOGIC CIRCUITS

Elena Feltri - Supervisor: Mario Caironi

Given the increased burden on healthcare workers in recent years, point-of-care medical devices for the gastrointestinal tract that require no external supervision could be pivotal in delivering fast diagnosis, monitoring, and treatment of numerous diseases. Over the past fifty years, the field of ingestible electronics has gained significant attention, with increasing research in the field and a number of devices already making their way onto the market. However, the widespread adoption of ingestible pills is hindered by significant safety concerns. Considering that these devices still rely on materials that are neither fully digestible nor biocompatible, retention hazards, where non-digestible parts can lead to complications such as blockages, irritation, or even perforation, are a prominent risk. Because of this, the use of ingestible devices in true point-of-care settings is not yet possible, and medical supervision during their administration, operation, and eventual retrieval is still needed. Edible electronics has emerged as the perfect candidate to both take the baton from ingestible electronics ideas and overcome their limitations by employing electronic devices comprised of food and food-grade materials, which are inherently safe upon ingestion, undergoing degradation within the body. This would overcome the need for recollection and envision a real point-of-care system where GI tract diagnostic, therapy, and monitoring can be made autonomously via ingesting an edible electronic device without hospitalization.

However, to establish a new paradigm in edible electronics that moves beyond silicon, it is necessary to begin with a fundamental reassessment of materials. This entails identifying substances that are edible and possess the electronic properties required for integration into functional devices. The list of regulated and widely used edible materials is huge, and many of these materials have already been used in green electronics applications. However, the lack of stable, good-performing semiconductors hinders progress in this field. Without these materials, edible transistors and electronic circuits cannot be achieved, limiting progress in this emerging field. To advance edible electronics and, in the future, enable the development of edible smart pills that could offer alternatives to traditional ingestible devices, finding reliable and stable edible semiconductors is a key challenge. This involves reassessing the performance of known edible semiconductors, enlarging the library of candidates and enhancing their performances, and exploring new materials that, while not typically associated with the food industry, have been proven safe for ingestion. This category includes materials used in cosmetics, like toothpaste and lipsticks, that, when used, come into contact with mucous membranes or are ingested and have thus already been tested for their toxicity upon ingestion, making them potential candidates for use in edible semiconductor applications.

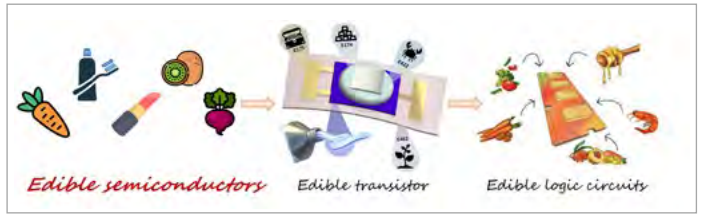

Fig.1 - Schematic representation of the experimental workflow of this dissertation: from the assessment of edible semiconductors, both food-based and daily-ingested materials present in cosmetics, to the development of fully edible transistors operating at low voltage (< 1 V), up to the fabrication and characterization of logic circuits.

This dissertation focuses on the development and characterization of edible semiconductors, transistors, and logic circuits, offering a pathway toward the next generation of edible electronic technologies. The research is structured into four experimental sections, addressing critical steps in the realization of edible devices, from the selection and optimization of edible semiconductors to the fabrication and demonstration of fully edible electronic components. The semiconducting properties of solution-processable food-based materials, namely carotenoids, are investigated to enhance their charge transport properties.

By applying a structure-processing-property approach, this work demonstrates significant improvements in the performance of carotenoid-based organic field-effect transistors (OFETs). The interplay between microstructure and charge transport is first investigated for beta-carotene, for which the optimized processing conditions yield field-effect mobilities two orders of magnitudes higher than the previously best-reported devices. The air stability of these devices is also addressed, resulting in progressively higher retention of the performances upon crystallization.

This approach is further extended to three other carotenoids: lutein, lycopene, and astaxanthin. The charge transport properties of devices obtained on the optimized microstructures yield in the case of lycopene-based OFETs mobilities comparable to beta-carotene-based ones and in the case of astaxanthin slightly lower mobilities, but displaying stable p-type charge transport over three weeks in air. These results establish carotenoids as promising candidates for future edible semiconductors.

Then, to widen the edible semiconductors library, the edibility and functionality of whitening pigments found in toothpaste are assessed. These pigments, insoluble in organic solvents and known for their semiconducting properties when deposited via thermal evaporation, are ingested daily due to accidental toothpaste ingestion and as a result of their whitening function. Thus, they are reassessed for their potential as edible semiconductors for edible transistors and logic circuits. In this framework, the blue Copper Phthalocyanine (CuPc) is demonstrated as a viable edible semiconductor, with daily ingestion quantified at around 1 mg/day, enabling the fabrication of the first fully edible p-type transistor with operating voltage < 1 V and with air-stability overcoming 1 year.

Afterward, Perchlorinated Copper Phthalocyanine ($Cl_{16}CuPc$), the most commonly used green pigment in toothpaste and mouthwash, is introduced as an edible n-type semiconductor, leading to the development of the first fully edible n-type transistor. The compatible fabrication process and comparable performances between the n-type and the p-type fabricated devices lead to the fabrication of edible complementary air-stable logic circuits, namely NOTs, a NAND, and a three-stage ring oscillator, which remain functional for over two months under ambient conditions.

The findings presented in this dissertation mark a fundamental advancement in the field of edible electronics, addressing critical challenges related to stability and functionality. The realization of fully edible semiconductors, transistors, and logic circuits shows the potential of this new field and paves the way for the next generation of edible devices for medical diagnostics, gastrointestinal monitoring, and beyond.

UNVEILING INTERFACIAL MAGNETISM IN HYBRID MAGNETIC HETEROSTRUCTURES WITH LINEAR AND NONLINEAR MAGNETO-OPTICAL TECHNIQUES

Alessandro Ferretti - Supervisor: Alberto Brambilla

The need to increase the performance of microprocessors and reduce their power consumption drives innovation at the lowest abstraction level. Thus, the focus is on finding an alternative to charge-based electronics and devising a radically new technology for nanoscale information transport. A viable approach is to replace or complement conventional charge-based electronics with spin-based electronics. This solution exploits the extra degree of freedom offered by the electron spin or rely on collective magnetic excitations called spin waves. Of particular interest are spin waves in antiferromagnetic materials because they open the possibility to process information at THz frequencies.
A novel approach for the excitation of spin waves in antiferromagnetic materials exploits the hybridized nature of the electronic states that form at the interface between organic molecules and antiferromagnetic materials, called *antiferromagnetic spinterface*. The idea is to couple light at visible wavelengths to the propagation of spin waves inside the antiferromagnet, using the molecules as a transducer. This would form the building block of a groundbreaking technology for information transport at the nanometer length scale and is the idea of the European H2020 project named SINFONIA, that constitutes the context for my PhD research activities.
The focus of my work is on low-dimensional magnetism, exploring interfaces in multilayered heterostructures involving ferromagnets, antiferromagnets and organic molecules. The magnetic materials I mainly worked with are transition metal ferromagnets like Fe, Co, Ni and their antiferromagnetic oxides: FeO, CoO and NiO. From the organic molecules side, I worked with C_{60}, FePc and CoTPP. All the previous compounds are evaporated by means of molecular beam epitaxy. Magnetic interfaces are the pillar for many physical phenomena and understanding and tailoring interfaces in magnetic heterostructures constitutes a fundamental step in the research and development of new technologies that leverage on magnetic materials. Despite strong interest in interfacial magnetism, selectively probing and investigating these elusive low-dimensional systems remains challenging.
During my PhD, I designed an experimental setup combining linear and nonlinear magneto-optical techniques to disentangle bulk and interface behaviors during magnetization reversal processes. This setup integrates the magneto-optic Kerr effect (MOKE) and magnetization-induced second harmonic generation (MSHG) techniques. A measure of MOKE allows to reconstruct the spatial evolution of the sample's magnetization at different values of an external magnetic field. While it provides information about the overall magnetization, the Kerr effect lacks selectivity to the interface. To specifically probe interfacial magnetism, I utilize MSHG. The interface selectivity of this nonlinear optical technique arises from space inversion symmetry breaking at the interfaces of centrosymmetric crystal structures, which characterize most of the materials I investigate. While time reversal symmetry is broken by the magnetization, its axial nature preserves space inversion symmetry. Therefore, the interface sensitivity is maintained in magnetic materials and simultaneous detection of MOKE and MSHG allows distinguishing the magnetic behavior of the bulk and the interface during magnetization reversal.
The experimental setup (Fig. 1) has a pulsed laser source combined with an optical parametric oscillator. An electromagnet capable of generating fields up to 1T is employed to drive the magnetization reversal of the sample along one axis.

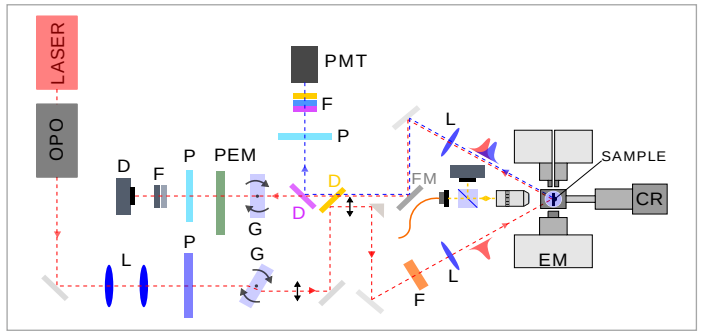

Fig.1 - Experimental setup. D: detector, F: filters, P: polarizer, G: glass, D: dichroic, L: lens, FM: flip mirror, EM: electromagnet, CR: Cryostat, PMT: photomultiplier tube.

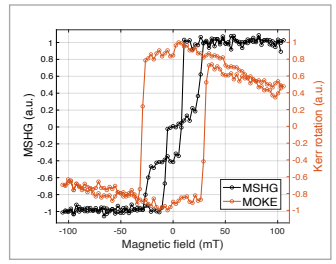

Fig.2 - MOKE and MSHG signals from MgO/Co/NiO/MgO.

Low-temperature measurements are performed with a closed-cycle cryostat reaching temperatures down to 10K. The signals are detected along two different paths: one for MOKE and the other for MSHG. MOKE is detected with a silicon diode by modulating the signal with a photoelastic modulator and demodulating it with a lock-in amplifier. MSHG is detected using a photomultiplier tube operating in photon counting mode. The laser is focused onto the sample using two configurations: either with lenses at a 25° angle of incidence or with a microscope objective. With the latter, the angle of incidence is tunable from normal incidence up to the limit of the objective's numerical aperture. The angle of incidence is adjusted by off-axis positioning of the beam on the objective's aperture. The setup also includes an imaging system with a CMOS camera and white light illumination. A custom-made software that I created automates the measurements.
One of the main results obtained with the completed setup was on a MgO/Co/NiO/MgO sample. The buried Co/NiO interface exhibits uncompensated Ni moments coupled at 90° with the Co moments due to spin-flop coupling. Combined MOKE and MSHG measurements revealed a different magnetization reversal at the interface compared to the bulk, see Fig. 2. This feature is attributed to the uncompensated Ni spins that act as a ferromagnetic layer at the Co/NiO interface and show a distinct magnetization reversal from the bulk Co, due to frustration.
Results were also obtained on a $CoO/Co/Al_2O_3$ multilayer, which exhibited exchange bias after field cooling. Temperature-dependent MSHG measurements tracked the evolution of the effective anisotropy axis at the Co/CoO interface. This suggests a possible origin for the sign change of the bias nearby the bocking temperature, which is a feature of this system. Furthermore, C_{60} evaporation onto the antiferromagnetic CoO modified the coercive field of the underlying Co layer and increased the blocking temperature of CoO. These results demonstrate the potential of MSHG and MOKE for probing magnetic interfaces and offer insights into phenomena such as spinterface-induced magnetic stabilization by distinguishing interfacial and bulk magnetization reversal.

GROUP IV BASED INFRARED PHOTODETECTORS FOR SWIR AND MIR DETECTION

Raffaele Giani - Supervisor: Daniel Chrastina

Short Wavelength Infrared Radiation (SWIR) detection has gained significant interest due to its diverse applications in automotive, biomedical, chemical detection, environmental monitoring, biology, astronomy, remote sensing, and imaging. Key advantages include enhanced penetration in scattering media such as fog, smoke, and rain, as well as the capability for night vision using atmospheric airglow. Germanium has emerged as a promising material for SWIR detection due to its CMOS compatibility, cost-effectiveness, and the ability to be directly grown epitaxially on silicon substrates. Ge-on-Si photodiodes exhibit high optical input power handling but their dark current remains a major challenge compared to InGaAs detectors, that are the state-of-the art for this spectral region. The dark current in semiconductor photodetectors is primarily influenced by intrinsic carrier concentration, which is significantly higher in Ge than in InGaAs due to the larger electron-effective mass of Ge. However, recent advancements in threading dislocation reduction and surface passivation have improved dark current performance. Additionally, tuning the doping profile of the silicon-germanium heterostructure presents a potential pathway for further optimization.

In the first part of this work, the analysis of the dark current of Ge-on-Si photodiodes was conducted. To carry out this analysis, a set of Ge-on-Si p-i-n structure were grown, by LEPECVD (Low-Energy Plasma Enhanced CVD) in the L-NESS facility, on silicon substrates with different doping levels.

Dark current in Ge-on-Si devices arises mainly from three mechanisms: diffusion, generation-recombination and trap-assisted tunneling. To evaluate the weight of these three different mechanisms in determining the dark current and how the doping profile can influence them, temperature dependent current-voltage (Figure 1.c) and capacitance-voltage (Figure 1.b) measurements have been performed. Then, the devices characterization has been completed by performing photocurrent measurements at different bias to estimate the responsivity (Figure 1.c) and his relation with the doping profile. Eventually, the specific detectivity has been estimated as a figure of merit of the photodetectors. The obtained results show that it is possible to reduce the dark current density by controlling the doping profile and that it is possible to design the photodiode to have the best trade off in terms of detectivity.

Mid-Infrared (MIR) detection plays a crucial role in identifying key chemical compounds such as carbon dioxide, methane, water, and nitrogen dioxide. Applications of MIR detection span medicine, astronomy, military technology, and environmental monitoring. Traditional MIR detection relies on semiconductor materials like InSb and nitrogen-cooled HgCdTe, which are expensive and incompatible with CMOS processing. Germanium-tin (GeSn) has emerged as a promising alternative for MIR detection, particularly for wavelengths around 3.3 µm, relevant for methane detection and food analysis.

GeSn alloys possess tunable bandgaps achieving group-IV epilayers featuring a direct bandgap in the MIR. An important advancement in GeSn-based MIR detection is the development of GeSn Avalanche Photodiodes (APDs), which utilize internal carrier multiplication for signal amplification. APDs offer superior sensitivity and improved signal-to-noise ratios, making them highly suitable for low-intensity infrared imaging and spectroscopy applications such as gas sensing.

The second part of this work focuses on the characterization of the germanium-tin alloy system, addressing its fundamental properties and critical challenges. Given that GeSn is an emerging material with a complex epitaxial growth process, the experimental determination of its optical bandgap and absorption coefficient is of particular interest. A methodology for estimating these optical properties is proposed, based on the measurement of reflectance (R) and transmittance (T) (Figure 2.a).

The focus then shifts to the fabrication of avalanche photodiodes, addressing the challenges associated with the GeSn alloy. One of the primary limitations is the thermal budget that GeSn can withstand, as any processing temperature exceeding 200°C leads to tin segregation, resulting in phase separation rather than a stable alloy. Another critical issue is the etching process, as GeSn is incompatible with fluoride-based chemistry and instead requires chloride-based etching techniques. The fabricated devices (Figure 2.b) were electrically characterized (Figure 2.c) at different temperatures, demonstrating the feasibility of designing avalanche photodiodes using germanium-tin.

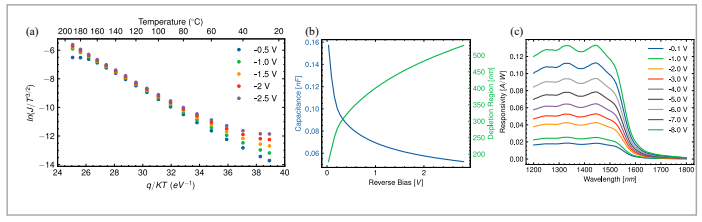

Fig.1 - (a) Arrhenius plot of reverese dark current for the sample grown on the heavily doped silicon substrate. (b) Capacitance-Voltage characteristics and the derived depletion region width for the same sample. (c) Responsivity measured for the sample on the intermediate doped silicon substrate.

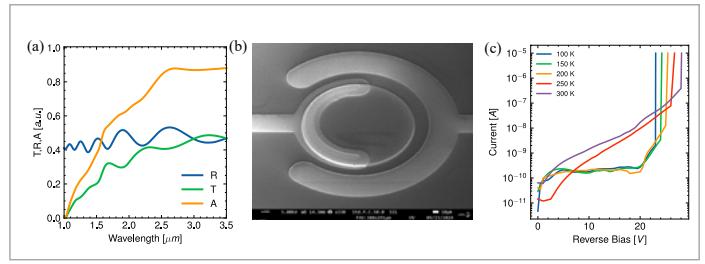

Fig.2 - (a) RT measurements and calculated A=T/1-R for a GeSn layer. (b) SEM image of a fabricated device. (c) Dark Current – Voltage characteristics at different temperatures for the Avalanche Photodiode.

PEROVSKITE DETECTORS FOR IONIZING RADIATION

Isabel Gonçalves - Supervisor: Annamaria Petrozza

In less than 100 years, X-ray interaction with matter was observed, characterized, optimized and transformed into a mighty tool to uncover hidden features to the visible eye. So profound was the quantity and quality of information it brought to the table, that this physical phenomenon was probably the fastest to move from pure research to implementation in our everyday lives. It's found everywhere: security, food inspection, quality control, let alone being the pillar of health monitoring, with accessible radiography and radiotherapy. Finally, this eccentric quality of light has given important contributions to research itself, granting a myriad of new techniques to dive deeper into the structure and function of new materials, paving the way for innovative technologies. Perovskite radiation detectors have shown be thousands of times more sensitive to X-rays than the detectors commercially available, while capable of detecting smaller X-ray radiation power (or more precisely, radiation dose). These two qualities together are crucial for healthcare, allowing more frequent X-rays to be taken without impacting the health of patients. This groundbreaking possibility is a result of the many qualities of perovskite materials. This class of ionically bonded semiconductors have attracted attention for their bandgap tunability, long carrier lifetimes, high defect tolerance and solution processable fabrication. Specifically for radiation detection, their large absorption coefficient allows efficient beam absorption even for low thicknesses, associated with the large-Z elements in their composition (Sn, I, Cs, Pb, Bi). Although these promising features have been arising over the last 15 years of perovskite research, their application to X-ray detectors is in a very early stage. Therefore, the first approach taken by the research community was to substitute the typical X-ray absorber (CdTe, Si, Se) for a perovskite material, keeping the same detector architecture. So far, 6 flat panel detectors have been demonstrated, all of them realized in a vertical structure (see Figure 1.a).

A NEW ARCHITECTURE

In this thesis, a new architecture of X-ray detectors is explored to verify whether it can be a real alternative in the future of ionizing radiation detection. In this geometry (see Figure 1.b), the absorber layer is irradiated vertically, while photogenerated carriers (electron and hole pairs) are collected laterally due to the coplanar electrodes. The decoupling of photon absorption and charge collection directions is a strategic choice due to the high X-ray absorption length. Since this value is in the order of mm, it results in loss of charge induction on the electrodes since this quantity is inversely proportional to the distance between them. Therefore, only in the co-planar architecture is possible to efficiently stop highly penetrating X-rays with 10^2 µm absorbers, while keeping the distance between the electrodes in the µm range, avoiding the operation at kV bias that all vertical detectors are obliged to for efficient charge collection. In this work, we transitioned from photolithographed metal electrodes to screen printed conductive pastes, with an increase in the performance of the devices.

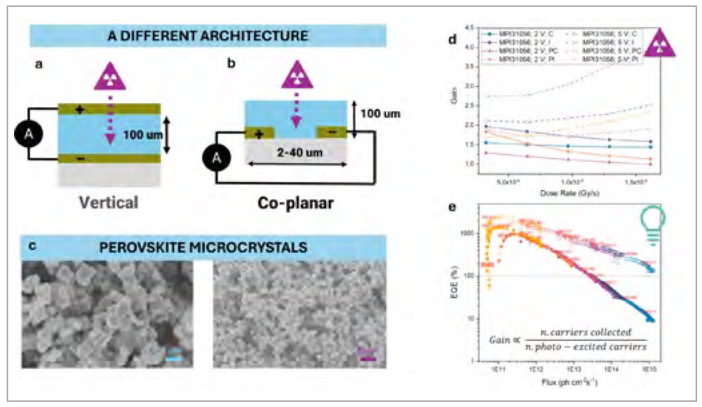

Fig.1 - a) Vertical X-ray detector architecture; b) Co-planar architecture; c) Different morphology of perovskite microcrystals; d) Example of Gain measured under X-rays for a subset of samples coated and non-coated with an organic electron acceptor; Figure e) EQE (equivalent to Gain) measured under visible light for two bias voltages, where it is evident its dependence on the flux (light intensity).

PEROVSKITE MYCROCRYSTALS

Flexibility is indeed an opportunity to be capitalized on. Curved detectors offer a better conformality to the X-ray wavefront, avoiding image quality loss at the edges of the detector. Flexible devices are also lightweight and less prone to breakage, opening the way for portable, in-situ imaging. To exploit this opportunity, a porous absorber layer composed of perovskite microcrystals of adjustable size and composition was used (see Figure 1.c). The microcrystals are blade coated to form a polycrystalline layer in contact with the co-planar electrodes. The structural and morphological properties of such microcrystals were correlated to the device performance under visible light and X-rays.

However, the co-planar architecture of Figure 1.b possesses its drawbacks. The non-uniform electric field upon bias adds complexity to the generation of signal (photocurrent) and hinders the carrier collection efficiency (CCE) resulting in a sensitivity drop. The CCE evaluation is well known for vertical detectors, but no physical model has been done so far for co-planar geometry, due to their 2-axis dependent electric field, which requires numerical methods. Therefore, the CCE was studied with finite element simulations to understand which parameters (geometrical and material-wise) had the most impact.

Although co-planar detectors suffer from lower sensitivity due the unfavourable electric field distribution, this is compensated by the existence of photoconductive gain. The gain originates from a strong unbalance in the transport properties of the photogenerated holes and electrons coming from different de-trapping times. This is especially relevant at low light fluxes, where one of the two carriers is deeply trapped and the other can drift under the external field. For a high flux radiation field, the traps can be filled and the gain eliminated. To bring the device to a stable operation where the gain doesn't depend on flux (and defect concentration), an electron acceptor was coated on the microcrystals to physically separates the two carriers (see Figure 1.e). In this way, the effect of the microcrystal's morphology and composition in the onset of gain was investigated. To bring this knowledge to the perovskite X-ray detectors field, a comprehensive measurement of the gain both under visible and X-rays was done, expressing it as function of the real excess carriers generated inside the semiconductor for a wide understanding comprising these two relevant colour palettes.

In summary, ionizing radiation detectors were developed both at the active material level and at the electrode geometry level. The latter comprised the integration on a favourable co-planar architecture. To tackle the non-uniform, low electric field in the architecture, we transitioned from lithographed to printed electrodes, showing an improvement of the signal correlated to a CCE enhancement studied with finite element simulations. Finally, through an experimental evaluation and analytical simulations, the gain in co-planar detectors was characterized for both visible and X-rays, bridging the gap between these two very different colours of light.

LABEL-FREE MULTIMODAL NONLINEAR OPTICAL IMAGING FOR CANCER CELL BIOLOGY

Francesco Manetti - Supervisor: Dario Polli

Biological microscopy has undergone a transformative evolution with the advent of advanced imaging techniques, offering unprecedented insights into cellular structures and functions at the molecular level. Fluorescence microscopy, the most widely used approach, provides high specificity and rapid imaging through engineered fluorescent labels. However, its reliance on exogenous markers alters native biological conditions, demands complex sample preparation, and limits its applicability in vivo. My doctoral research focused on overcoming these constraints by leveraging label-free nonlinear optical microscopy in a multimodal framework.

Nonlinear optical techniques, enabled by ultrafast laser sources, exploits the interaction of pulsed laser beams with biological matter to generate diverse nonlinear signals rich in biochemical information. I have focused my research on coherent Raman scattering and multiphoton processes to probe molecular composition and cellular energy metabolism, offering a powerful toolset for diverse biomedical applications. In cancer research, we identified intrinsic, early-stage markers of therapy-induced senescence (TIS) in human hepatic cancer cells (HepG2), an elusive cell state linked to treatment resistance, cancer dormancy, and relapse. Using stimulated Raman scattering (SRS), two-photon excited fluorescence (TPEF), and coherent anti-Stokes Raman scattering microscopy (CARS), we visualized and quantified TIS biomarkers at early stages, monitoring their progression over time (Fig. 1). This work showed the potential of nonlinear optical techniques in cancer therapy screening and the development of novel anticancer treatments.

To further demonstrate the generalizability of these biomarkers, we used machine learning and deep learning algorithms for image classification to identify TIS and control cancer cells. Our ensemble model, integrating seven pre-trained classification networks, taken from literature, with additional fully connected layers, achieved over 90% classification accuracy. This automated approach offered a fast, unbiased, and precise method for identifying TIS cancer cells, with promising applications in clinical and preclinical diagnostics.

In drug delivery research, we investigated the internalization of novel upconverting nanoparticles within HeLa cells. These NIR light-controlled nanocarriers hold promise for non-invasive drug delivery with high spatiotemporal precision. TPEF microscopy confirmed successful uptake, demonstrating their biocompatibility and potential in targeted biomedical applications.

In immunology, we used SRS microscopy to analyze the diverse immune responses of murine macrophages to biochemical and mechanical stimuli in vitro. While macrophage polarization can be identified using pre-defined markers, label-based approaches cannot recapitulate the complexity and the dynamism of the polarization spectrum within the tumor microenvironment. This demonstrated the potential of label-free approaches to investigate the role of macrophage polarization in tumor progression, providing deeper molecular insights into macrophage response.

To fully exploit the potential of multimodal nonlinear microscopy, we designed and developed a novel optical imaging platform. The system is powered by a picosecond pulsed, fiber-based, dual-output laser source which can be rapidly tuned over a wide range of wavelengths. We integrated the laser in a custom-built microscope, which features rapid-scanning galvanometric mirrors, a long-travel XYZ motorized stage, a multi-channel detection unit for simultaneous signal acquisition, both in trans- and in epi-detection modalities, and a top-stage incubator for live-cell imaging. Designed for diverse applications, this compact, versatile system is poised to address ground-breaking biomedical challenges, such as the continuous, non-destructive monitoring of patient-derived tumoroids with subcellular detail. This capability would present a powerful alternative to animal models for preclinical cancer drug testing, paving the way for more effective and personalized cancer therapies.

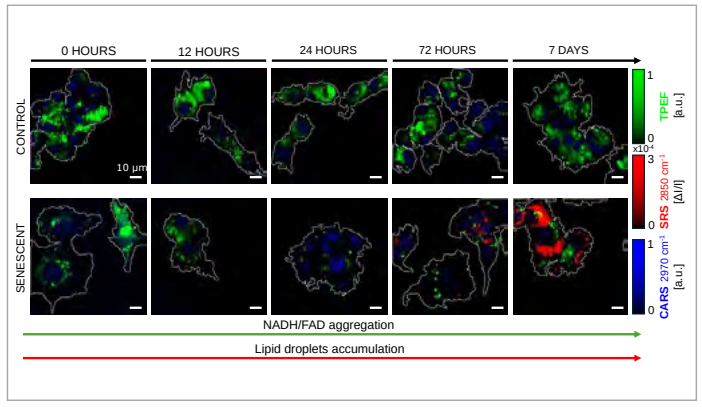

Fig.1 - Label-free multimodal nonlinear optical images of control and TIS HepG2 cells. The images were collected over a period ranging from 0 hours to 7 days of culture. TPEF signals from NAD(P)H and FAD are shown in green, 2850 cm–1 SRS signals from lipids are shown in red, and 2970 cm–1 CARS from deoxyribose in nuclei is shown in blue. TPEF microscopy visualizes severe rearrangements in the mitochondrial network, starting early treatment time. SRS microscopy evidences a strong and clear accumulation of lipid vesicles starting 72 hours of treatment.

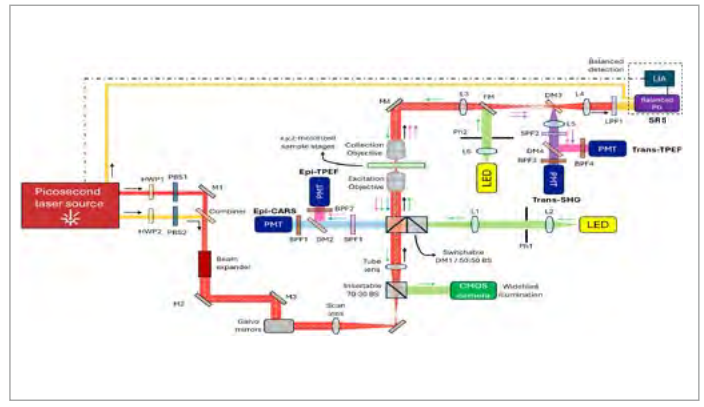

Fig.2 - Optical scheme of the multimodal nonlinear microscope. HWP: half-wave plate; PBS: polarizing beam splitter; M: mirror; L: lens; DM: dichroic mirror; SPF: short-pass filter; BPF: band-pass filter; LPF; long-pass filter; Ph: Pinhole; LIA; lock-in amplifier. Yellow line: Stokes beam. Red line: pump beam. Green line: white light. Cyan line: coherent anti-Stokes Raman scattering. Pink line: two-photon excited fluorescence. Purple line: second-harmonic generation.

ALL-OPTICAL CONTROL OF LIGHT WITH DYNAMIC NONLOCAL DIELECTRIC METASURFACES

Akturk Mert - Supervisor: Margherita Maiuri

Achieving light manipulation at higher speeds and subwavelength scales is essential for modern technologies, which prioritize precision, efficiency, and miniaturization in integrated photonic devices. However, conventional optical elements such as lenses and waveplates rely on propagation through optically thick media, leading to bulky and less efficient designs. Moreover, their capability to manipulate electromagnetic waves, limited by the properties of natural materials, restricts the range of functionalities that can be implementable. This is inherently constrained by electronic modulation limitations, creating a bottleneck in the GHz speeds. Over the past two decades, significant advancements in nanofabrication techniques have boosted the emerging field of nanophotonics. This field has enabled the transition of well-established technologies from controlling radio and microwave frequency radiation to the visible and near-infrared (NIR) range of the electromagnetic spectrum, thus radically changing the perspective of the optics field. To address these challenges, significant interest has shifted toward developing artificial materials known as *metamaterials* and their more recent two-dimensional counterparts, *metasurfaces*. These consist of quasi-2D arrangements of nanostructures, packed in arrays with sub-wavelength configurations. The response of these materials to electromagnetic radiation is determined by the resonances of their constituent building blocks, known as meta-atoms. Such nanostructures can resonantly capture the light and re-emit it with a pre-defined phase, polarization, modality, and spectrum, thus allowing the sculpting of light waves within lengths of a few hundreds of nanometers. More specifically, they can be implemented for various functionalities from beam steering, wavefront manipulation and polarization control to more exotic applications as invisibility cloaking and negative refraction. Furthermore, recent studies have increasingly focused on active (reconfigurable) metasurfaces.

Unlike passive metasurfaces, which have optical functionalities fixed during the design phase and set in stone during the fabrication process, dynamic metasurfaces incorporate tunable elements, enabling real-time adjustment of their optical response through electrical, thermal, mechanical or optical stimuli. Furthermore, nanophotonic structures serves as an excellent platform for exploiting nonlinear phenomena due to their ability to concentrate light and enhance fields at subwavelength scales through resonances. As a result, significant interest has emerged in enhancing modulation speed via nonlinear effects, leading to the development of ultrafast "all-optical" metasurfaces. This all-optical approach relies on manipulating light with light: by inducing the third-order nonlinearity of the material—such as transient, intensity-dependent changes in the refractive index via a control laser pulse—a second pulse experiences the modified optical response of the material within the characteristic timescale of the light-matter interaction, typically in the order of tens of femtoseconds to several tens of picoseconds. This gives rise to a new class of spatiotemporal nanostructures in which time, akin to space, acts as a new degree of freedom for controlling the metasurface behavior. The work presented in this thesis contributes to the ongoing efforts to achieve a comprehensive picture of ultrafast nonlinear effects in nanostructured optical materials. In this framework, understanding the mechanisms dominating the photo-induced modification of matter and their impact on the optical response of nanostructured systems are discussed. To unveil the principal physical processes, experimental investigations via polarization-resolved pump-probe spectroscopy and ultrafast Fourier microscopy methods are exploited and the results are complemented by an accurate predictive model based on a multi-physics approach. First, the polarization-resolved spectroscopy technique is utilized to characterize dielectric metasurfaces for manipulating light polarization, enabling both high-contrast polarization-selective switching and transient modulation in dichroic and birefringent properties. Consequently, the capabilities of nonlinear all-dielectric AlGaAs metasurface (Fig. 1a) were tested, achieving giant transient dichroic modulations with a reflectivity modulation of up to $\Delta R/R \approx 470\%$ in TM mode (Fig. 1b) and inducing a relative phase shift of up to ($\Delta\varphi = \pi/2$) between the orthogonal TE and TM modes at the reflected polarization ellipse (Fig. 1c). Moreover, we leverage the capability of metasurfaces to engineer scattered light, tailoring the phase profiles to shape optical wavefronts on demand. While wavefront engineering has been largely demonstrated, achieving such control dynamically in the ultrafast regime remains more challenging. The common working principle among the reported studies in this thesis relies on the intriguing concept of photo-induced spatial inhomogeneities. This results from the non-uniform energy distribution shaped by the astigmatic profile of the pump pulse, which creates a gradient in the photo-induced hot-carrier profile. To investigate the ultrafast response of a silicon-based nanowire metasurface we utilize our custom-built ultrafast k-space apparatus which combines a standard pump-probe and a Fourier imaging detection. The nanostructure is excited by an astigmatic pump pulse, which is spatially elongated over 4 mm along the nanowires' direction (y-axis in Fig. 2a). This excitation generates a spatial gradient in the permittivity variation along the transverse direction (x-axis), evolving over time due to ultrafast hot-carrier relaxation. A delayed broadband probe pulse, incident normally on the metasurface, undergoes temporal modulation of its spatial phase profile, leading to changes in the probe wavevector components. Transient k-space maps are recorded (Fig. 2b) using a camera at a chosen probe wavelength, revealing the ultrafast onset of transmitted wavevector deflection from normal incidence ($k_x = 0$). Taken together, the findings presented in this thesis highlight how the combination of advanced experimental techniques, supported by theoretical methods, can open new routes for understanding and effectively controlling light-matter interactions. This approach not only maximizes the potential of existing technologies but also reveals novel and promising routes for further exploration.

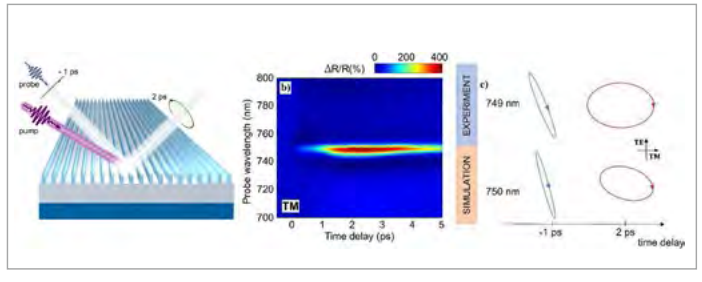

Fig.1 - (a) AlGaAs nanowires with the probe pump-probe scheme (b) experimental transient dichroism map, and (c) dynamical polarization ellipse reconstruction.

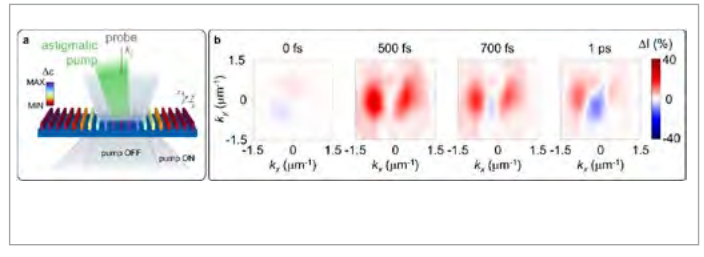

Fig.2 - (a) Scheme of the ultrafast k-space experiment on the Si nanowire metasurface representing the transient wavefront deflection. Colored gradient across the nanowires represents the pump induced permittivity variation Δε. (b) Differential transmission maps (k_x, k_y) for a series of pump-probe delays.

THE PATH TOWARDS ATTOCHEMISTRY: EXPLORING ULTRAFAST MOLECULAR DYNAMICS FROM XUV-IR TO UV-XUV PUMP-PROBE TECHNIQUES

Daniele Mocci - Supervisor: Rocío Borrego Varillas

My PhD research focused on exploring ultrafast dynamics in molecular systems, evolving from XUV-IR to UV-XUV pump-probe techniques. The aim was to uncover electronic and vibrational phenomena occurring on attosecond to femtosecond timescales, contributing to the emerging field of attochemistry. The development of attosecond science has revolutionized our understanding of ultrafast molecular processes. With temporal resolution on the order of tens of attoseconds (1 as = 10-18 s) this field has allowed us to observe and manipulate electron dynamics, previously inaccessible. Central to this progress is the advancement of XUV-IR pump-probe methods, enabling precise exploration of ultrafast processes. In this scheme, an attosecond XUV pulse ionizes the target, creating a superposition of cationic states, while a time-delayed IR pulse probes the resulting dynamics by inducing transitions between these states.

A key achievement in my work was the design and optimization of an XUV-IR pump-probe beamline, which facilitates the investigation of electron-nuclear coupling in complex organic molecules. One of the specific scientific cases that I studied was the effect of halogen substitutions on small amino acids. We investigated phenylalanine and its halogen-functionalized derivatives, where a hydrogen atom in the para position of the benzene ring was substituted with a fluorine, chlorine, or iodine atom. Figure 1 shows the time-resolved signals tracking ion yield variations for key molecular fragments as a function of pump-probe delay. This method reveals how different halogen substitutions affect fragmentation pathways and charge localization.

These experimental results were supported by computer simulations, which allowed us to attribute the ultrafast dynamics to a barrier-less decay mediated by conical intersections.

Iodine accelerates relaxation due to the heavy-atom effect (magenta curve), while chlorine induces slower transitions through stronger electronic and vibrational couplings (pink curve). Fluorine, due to its small size, does not significantly influence this dynamic (violet curve).

The journey toward attochemistry requires the ability to study and control chemical reactions at the attosecond timescale. To this end, a central theme of my Ph.D. has been the design and construction of a UV pump-XUV probe beamline, which integrates sub-3 fs UV pulses with attosecond XUV pulses. This setup allows for the study of UV-excited neutral molecules, marking a significant step toward real-time observation of ultrafast photo-chemical processes. The UV pulses are generated via resonant dispersive wave emission in hollow capillary fibers, demonstrating broad tunability (200 to 350 nm) and few-fs pulse duration. For the XUV probe pulses, I demonstrated for the first time efficient isolated attosecond pulse generation in an extended medium by driving high-order harmonic generation with few-fs IR pulses in a semi-infinite gas cell. Theoretical simulations, performed by our collaborators, showed a reshaping of the driving pulse that enhances time-gated phase matching. This breakthrough represents a significant step forward in the broader adoption of isolated attosecond pulse technology, providing a versatile new tool adaptable to a range of experimental setups.

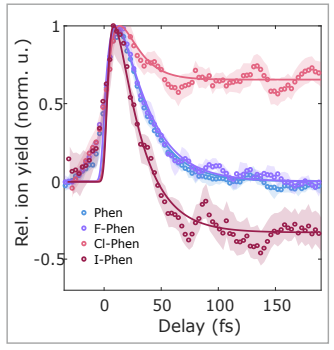

Fig.1 - Relative ion yield of the fragment (M-COOH)2+ with the corresponding fit for the four different compounds (phenylalanine and its halogen functionalization: 4-fluoro-phenylalanine, 4-chloro-phenylalanine, 4-iodo-phenylalanine)

My work includes proof-of-concept experiments conducted with this UV-XUV beamline, showing its capability to resolve femtosecond-scale dynamics in model systems. Figure 2 displays the experimental instrumental response function, demonstrating a resolution of 3 fs, a remarkable result for this type of beamline—one of the first to achieve this resolution for femtosecond UV pulses. Preliminary studies on pyrazine, a prototypical molecule with significant relevance across various fields due to its unique structural and chemical properties, showcase the system's exceptional temporal resolution. From a photochemical perspective, pyrazine is one of the most extensively studied molecules as it serves as a model system for investigating non-adiabatic dynamics involving ultrafast transitions through conical intersections. In these studies, the few-femtosecond UV pulses excite the molecule in its neutral form, while attosecond pulses project the excited states into the continuum by ionizing the molecule. This process enables the generation of time-resolved photoelectron spectra, providing a detailed, time-dependent map of the ultrafast dynamics at play.

These initial results validate the robustness of the setup and its potential for a wide range of molecular targets. The integration of UV excitation and XUV probing, along with experimental and theoretical advancements, sets new benchmarks in attochemistry.

The transition from XUV-IR to UV-XUV techniques marks a significant step toward real-time control of chemical reactions at the attosecond scale. The research presented here lays the foundation for future studies focused on mapping electron dynamics in increasingly complex molecular systems. It also highlights the technological and conceptual advancements needed to achieve the ambitious goal of attochemistry: the direct manipulation of molecular behavior at the electronic level. This work paves the way for investigating light-matter interactions beyond traditional ultrafast spectroscopy. Future directions include applying these techniques to larger organic molecules, offering insights into charge transport, excited-state dynamics, and energy redistribution processes critical to chemical physics and material science.

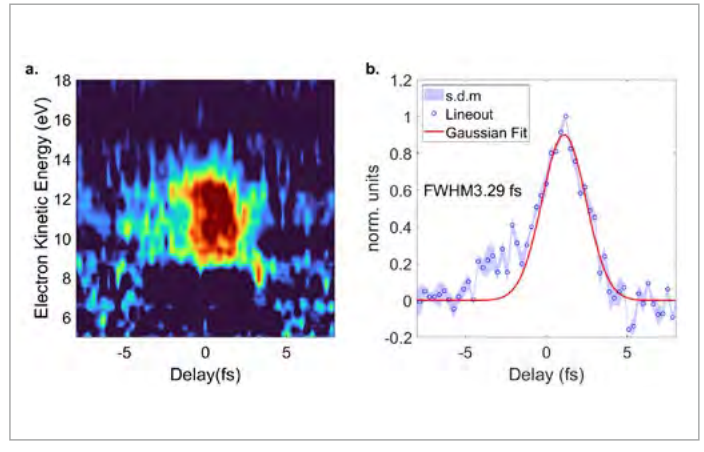

Fig.2 - Photoelectron UV+XUV spectrogram in Argon. B. Lineout of the spectrogram highlighting a FWHM of 3.3 fs, corresponding to the instrumental response function of the setup.

TUNABLE FEW-CYCLE UV PULSES FOR ATTOSECOND SPECTROSCOPY

Marta Pini - Supervisor: Maurizio Reduzzi

Following the very first steps of photoinduced electronic movements inside a molecular system is of crucial importance to understand how it chemically behaves, changes, and evolves upon radiation absorption and how the molecular structure subsequently rearranges on longer temporal scales. The study and the understanding of such electron dynamics in molecules of increasing complexity is the first step towards the possibility of controlling and even engineering the molecular response, enabling a variety of technological applications. This opportunity emerged with the birth of attosecond science, and thus the availability of laser pulses with a temporal duration in the order of hundreds of attoseconds, short enough to track such ultrafast electronic movement.

Since most of the organic compounds present strong electronic excitations in the Deep Ultraviolet (200 nm - 300 nm) and Ultraviolet (300 nm - 400 nm), ultrashort, few-cycle laser pulses in these spectral ranges are needed to resonantly excite these molecular systems, triggering electronic coherences and ultrafast charge dynamics, which happen on temporal scale shorter than hundreds of femtoseconds. Such pulses, employed to initiate the dynamics, can be combined with attosecond pulses, used to sample the evolution of the induced process on its proper time scale. Performing this kind of experiments maintaining few-fs temporal resolution is a challenging task.

Resonant Dispersive Wave (RDW) emission in Hollow Capillary Fibers (HCF) filled with noble gases represents a breakthrough in the generation of few-femtosecond ultraviolet pulses. This innovative approach based on soliton dynamics in optical waveguides surpasses the bandwidth constraints of nonlinear crystals, while offering higher conversion efficiencies and output pulse energies compared to third harmonic generation in gases. Additionally, it provides the advantage of spectral tunability. RDW emission has already been demonstrated as a source of tunable pulses with central wavelengths spanning the Vacuum Ultraviolet, Deep Ultraviolet, and Ultraviolet ranges, achieving few-femtosecond durations and microjoule-level energy per pulse.

The aim of this thesis is the realization of an RDW-UV-pump XUV-probe spectroscopy beamline to perform Time-Resolved Photoelectron Spectroscopy (TR-PES) experiments on gaseous molecular target. The first step towards this task is the design and the implementation of a compact setup to generate UV pulses exploiting RDW emission in gas-filled HCF driven by infrared laser pulses, based on numerical simulation of pulse propagation in gas-filled capillaries. Their complete and direct temporal characterization via an all-in-vacuum Self-Diffraction Frequency Resolved Optical Gating has also been done, importantly for time-resolved spectroscopic applications. To guarantee the generation of dispersion-free UV pulses, the employed setup configuration exploited decreasing gas pressure gradient in the fiber, pumping gas at fiber input and evacuating its output, and thus directly connecting the capillary to the vacuum chamber where the characterization is performed. The direct characterization of the obtained pulses confirms the exquisite temporal properties of RDW, retrieving a temporal duration below 3 fs in the whole explored tuning range, between 250 nm and 350 nm central wavelength. The RDW-tunability in the DUV and UV, obtained using neon as nonlinear medium filling the HCF is reported in panel (a) of Fig.1, while panel (b) shows the reconstructed temporal profile of the pulse at 298 nm and its comparison with the one obtained from simulations.

In addition to the generation and the direct temporal characterization of RDW pulses, we also developed an innovative and flexible pump-probe beamline, able to combine the just described source of sub-3 fs pulses tuneable in the Deep Ultraviolet and Ultraviolet spectral regions and hundreds of nanojoule of energy per pulse on target, with attosecond XUV pulses, generated in a Semi-Infinite Gas Cell setup. Such beamline aims at studying via time-resolved photoelectron spectroscopy the aforementioned ultrafast molecular dynamics induced by the absorption of UV radiation in molecules of biological relevance and optoelectronic interest, such as donor-acceptor systems, probing them with XUV pulses.

A first in-situ characterization of the instrumental response function (IRF) of the setup has been performed via cross-correlation in noble gas of the XUV and UV pulses. Sideband formation upon two-colour ionization of argon revealed the capability of the beamline to perform experiments pushing the temporal resolution up to 3.3 fs. In addition to that, the first UV-pump XUV-probe measurement on molecular targets has been carried out on pyrazine, which represents an optimal benchmark molecule since it presents high absorption cross section in the Deep UV and in the UV spectral regions, and it has already been extensively studied both theoretically and experimentally with a temporal resolution of tens of femtoseconds. In this thesis, we carried out time-resolved photoelectron spectroscopy experiments with an unprecedented temporal resolution of approximatively 5 fs. The 2D map in Fig.2c shows the time-resolved photoelectron signal of the molecule, when the system is resonantly pumped at 267 nm (Fig.2a) and probed with XUV radiation at 22 eV (Fig.2b). This time-resolved signal gives information regarding the timescale of ultrafast nonradiative relaxation processes in the molecule in the first fs after the UV excitation.

The full beamline capability of pump-wavelength tunability, needed to match specific molecular excitations, and the combination of such pulses with isolated attosecond pulses, will be exploited to follow in real time the UV-induced electron dynamic of donor-acceptor systems for opto-electronic applications.

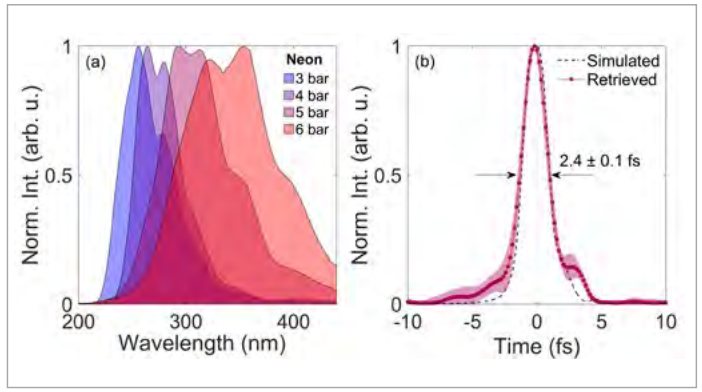

Fig.1 - (a) Wavelength tunability of the RDW pulses generated in Neon-filled HCF, as a function of the gas pressure at fiber input. (b) Dotted line and s haded a rea represent t he t emporal p rofile o f t he p ulse at 2 98 nm, retrieved from SD-FROG trace reconstruction. Dashed line represents the simulated temporal profile.

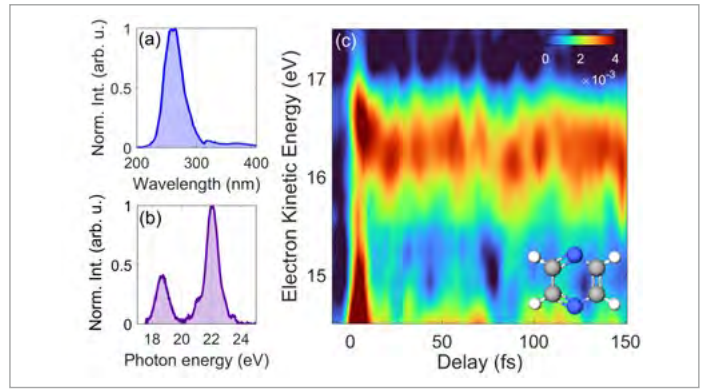

Fig.2 - Spectra of (a) UV pump pulses and (b) XUV probe pulses used in TR-PES on pyrazine. The XUV one is obtained by filtering the full harmonic spectrum with a tin filter. (c) Time-resolved photoelectron spectrum of Pyrazine, and pyrazine molecular structure (blue for nitrogen, grey for carbon, and white for hydrogen)

DEEP LEARNING ANALYTICS AND INTERPRETABILITY OF MOLECULAR LEVEL THROUGH SYSTEM LEVEL BIOPHOTONICS DATA

Salvatore Sorrentino - Supervisor: Dario Polli

My doctoral research focuses on integrating deep learning with biophotonics to address long-standing challenges in molecular characterization, spectral analysis, and cell state classification. Raman spectroscopy, a widely used non-invasive optical technique, provides detailed molecular fingerprints of biological and chemical samples. However, its interpretation remains complex, limited by factors such as overlapping spectral features, noise interference, and the high dimensionality of vibrational spectra. Traditional computational approaches, including Density Functional Theory (DFT) calculations, offer a theoretical solution but are computationally expensive and impractical for large-scale or real-time applications. My work bridges this gap using machine learning frameworks that enhance spectral prediction, improve interpretability, and automate data-driven analysis of biomedical imaging datasets.
One of the research projects in my PhD is the development of Mol2Raman, a graph-based neural network (GNN) designed to predict spontaneous Raman spectra directly from molecular structures. Unlike conventional approaches that rely on quantum chemistry simulations, Mol2Raman utilizes Graph Isomorphism Networks with Edge Features (GINE) to efficiently encode atomic and bond-level interactions. This allows the model to learn complex molecular vibrational properties, providing accurate predictions of both peak positions and intensities across diverse chemical datasets.
Benchmarking against existing machine learning models, Mol2Raman demonstrates superior performance in generalization tasks, accurately predicting spectra for structurally diverse and previously unseen molecules.
The model predictive capability significantly accelerates research in chemistry, materials science, and biomedical diagnostics. Moreover, its ability to replace expensive DFT-based calculations presents a scalable and efficient solution for applications where real-time spectral analysis is essential. Figure 1 A) illustrates the architecture of Mol2Raman, while Figure 1 B) shows the predicting performance of the network against a benchmark model, which prove its reliability as predictive model. Another research in my PhD journey involves the development of deep learning-based models for cellular state classification, specifically in the context of senescence detection. Cellular senescence, a critical process in aging and cancer progression, represents a complex biological state characterized by irreversible cell cycle arrest, morphological changes, and metabolic alterations. Accurately identifying senescent cells in heterogeneous populations remains a major challenge for biomedical research, particularly in cancer studies where therapy-induced senescence (TIS) contributes to tumor dormancy and resistance to treatment.
To address this, I developed a multimodal deep learning ensemble framework that integrates nonlinear optical (NLO) microscopy, Raman spectroscopy, and hyperspectral imaging data to classify senescent cells with high accuracy. By combining morphological features with spectral signatures, the model achieves robust classification across different cellular phenotypes, distinguishing senescent from proliferative cells based on key molecular and structural biomarkers.
Specifically, this model leverages on a combination of Transfer Learning and Ensemble Learning frameworks, which allow to reach a classification accuracy larger than 90%. In addition, I also inspect which features in the input images are the most significant in distinguishing between images of senescent cells and proliferating ones. To extract these features, I used the Grad-CAM approach, building the so-called heatmaps, which highlight the most important pixels in the input channels that activated the neural network to separate between the two classes of cells. Figure 2 A) and B) show that, when the predicted class is 'Senescence', the activated pixels (bottom panel) correspond to the pixel locations of mitochondria and lipid droplets (upper panel), whereas there is no activation of pixels when the predicted class is 'Control' (B).
The implications of this work extend beyond basic biological research, providing a powerful tool for clinical applications in cancer therapy assessment.
By enabling fast and automatic detection of cellular senescence, the proposed methodology opens new possibilities to evaluate the effectiveness of anticancer therapies in real-time.
In conclusion, my doctoral research highlights the impact of artificial intelligence in Raman spectroscopy and biophotonics, proving how deep learning can enhance spectral analysis and cellular state classification. The development of Mol2Raman provides a practical solution for accurate and fast Raman spectral prediction, avoiding computationally expensive methods. Likewise, my work on senescence classification showcases the potential of AI-driven models in biomedical imaging, offering new insights into senescence discovery. By integrating deep learning with experimental biophotonics, this research contributes to advancing molecular characterization and medical diagnostics, bridging the gap between optical spectroscopy and intelligent data analysis.

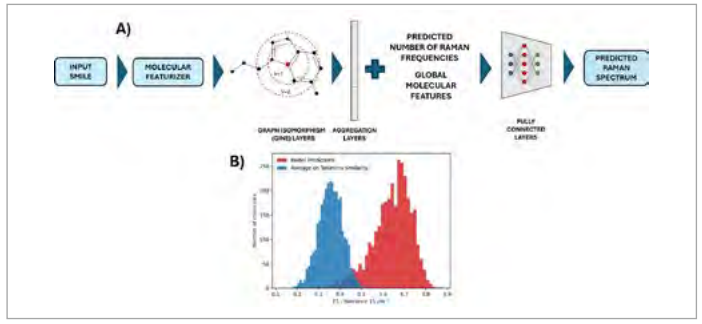

Fig.1 - A) Schematic representation of Mol2Raman architecture; B) Mol2Raman performance (red) against a benchmark model (blue)

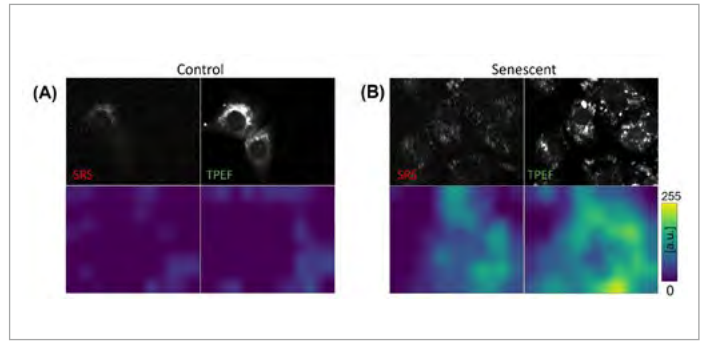

Fig.2 - Heatmap and corresponding optical signal for a control cell (A) and a senescent cell (B)

MULTISCALE OPTICAL IMAGING IN PLANT BIOLOGY FROM MOLECULAR TO MACROSCOPIC STRUCTURES

Giorgia Tortora - Supervisor: Andrea Bassi

As the world moves toward greater sustainability, the need for more sustainable agricultural practices has become increasingly evident. This requires cultivation methods that minimize environmental impact, reduce waste and enhance product quality. Achieving this goal begins with understanding the mechanisms underlying plant growth and responses to external stimuli. This understanding allows us to optimize growth conditions and select effective cultivation strategies.

A technique to investigate plant behaviour is required. Research has shown that calcium (Ca^{2+}) acts as a second messenger in plants, playing a key role in developmental mechanisms and signaling events in response to external stimuli. Thus, studying Ca^{2+} dynamics is a valuable approach to investigating plant behaviour. Specifically, calcium imaging, a technique that employs fluorescence imaging to optically measure Ca^{2+} levels within plant tissues, stands out. This method uses fluorescent Ca^{2+} indicators that are introduced into the plant and emit a detectable fluorescence signal upon binding with calcium ions. My PhD research focused on implementing this technique at microscopic and macroscopic scales.

At the microscopic level, a light-sheet fluorescence microscopy (LSFM) setup was employed to study root hair growth in plants (Fig. 1A). Root hairs are single cells that elongate from the plant root and are fundamental for nutrient uptake. Their proper growth is essential for the healthy development of the plant. Previous research has shown that healthy root hairs exhibit a tip-focused calcium gradient that oscillates in time with a characteristic frequency. Analysing Ca^{2+} dynamics at the root hair tip is, therefore, a valid method for evaluating the health of a mutated plant and assessing the role of specific genes in growth mechanisms.

Specimens of *Arabidopsis thaliana*, the model plant, with a complete genetic background, and specimens with a specific gene mutation were investigated. In mutant plants, an alteration in growth rate accompanied by a disruption of the tip-focused Ca^{2+} dynamics was observed (Fig. 1B). Performing Fourier analysis, a difference in the oscillation frequencies was identified (Fig. 1C). This led to the conclusion that the mutated gene plays a role in the proper growth of root hairs.

The focus then shifted to macroscopic investigation of plants, analysing their reaction to external stimuli. Plants are sessile organisms that cannot move. To defend themselves from external challenges, they have developed sophisticated mechanisms that allow them to perceive external stimuli and adapt to the environment. One of these mechanisms is the propagation of long-distance Ca^{2+} waves, which transport information from the site of the stimulus to distal tissues. To study long-distance Ca^{2+} signaling, it is necessary to move beyond single microscopic structures and observe the plant at the whole-organism level. Until now, this has been achieved using low-magnification objectives.

This approach has a major limitation: the field of view (FOV) provided by low-magnification systems is small and does not allow for the observation of entire adult plants. This limitation becomes even more evident in the context of climate change, which requires moving beyond the study of the model plant to investigate plant species of economic interest characterized by large dimensions. My PhD research aimed to overcome this constraint by developing a system that enables the study of adult plants. The developed imaging system consists of two identical units arranged at a 90-degree angle (Fig. 2B). Each arm provides an illumination field with a 20 cm diameter, while the detection unit captures images from a comparable area, making it possible to perform Ca^{2+} imaging on the entire shoot of adult crop-like plants. Furthermore, the dual-view feature, in combination with the use of 3D-printed rhizoboxes, pots with a transparent wall that facilitates root visualization (Fig. 2B), allows simultaneous imaging of both shoot and root.

Using this setup, experiments were conducted on adult *Nicotiana benthamiana* plants expressing the GCaMP3 intensiometric calcium indicator. Samples were subjected to various stimuli, including mechanical pressure, burning, and submersion. The results demonstrated that plant responses vary depending on specimen size and stimulus intensity. An example is presented in Figure 2, which shows the response of a 7-leaf-old *N. benthamiana* plant to leaf burning. In response to the stimulus, in addition to a local increase in calcium level, the systemic propagation of a calcium wave reaching distal leaves was observed (Fig. 2A-C).

In conclusion, the developed macro-imaging system marks a significant advancement in plant imaging technology. It enables comprehensive, non-invasive fluorescence imaging of both shoot and root systems in adult plants under physiological conditions, providing a powerful tool for studying long-distance Ca^{2+} signaling across different plant species.

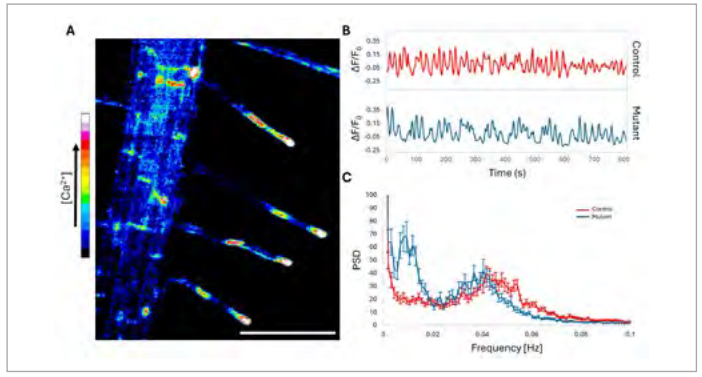

Fig.1 - (A) Maximum intensity projection (MIP) of a single time point stack of a control Arabidopsis specimen expressing the intensiometric Ca2+ indicator R-GECO1. Several root hairs are imaged at the same time thanks to the use of LSFM. Scale bar = 100 µm. (B) Ca2+ dynamics over time in a control and a mutant root hair evaluated as normalized R-GECO1 fluorescence intensity (ΔF/F0). Sampling time: 3 seconds. Measure repeated 270 times. C) Mean power spectral density (PSD) obtained with Fourier analysis.

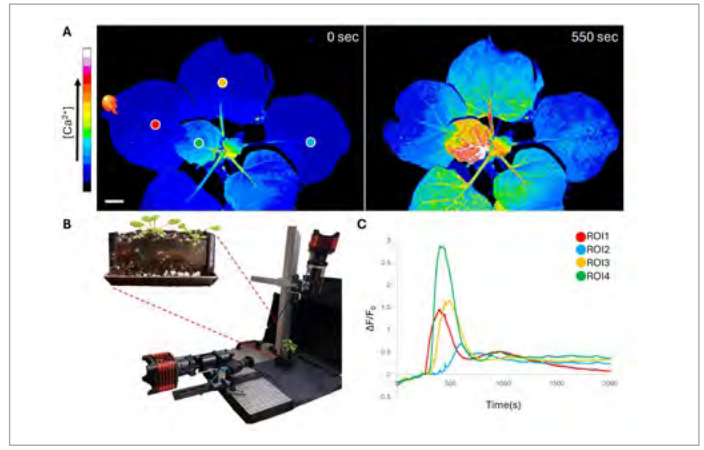

Fig.2 - A) Images of a 7-leaf-old N. benthamiana plant before and after leaf burning. Scale bar: 1 cm. B) Developed macro-imaging system with an example of 3D-printed rhizobox. C) Normalized GCaMP3 fluorescence intensity (ΔF/F0) in local and distal leaves.

ULTRAFAST OPTICAL SPECTROSCOPY: FROM CLASSICAL TO QUANTUM LIGHT

Lorenzo Uboldi – Supervisor: Giulio Cerullo

The developments in laser physics and nonlinear optics of the last few decades have allowed generation of intense ultrashort light pulses with duration of the order of few femtoseconds. Such pulses have been used to develop time-resolved spectroscopic techniques, as pumpprobe or fluorescence lifetime spectroscopy. Such methods have been extensively applied to the study of the dynamics of electronic excited states in matter. During my PhD research, I had the chance to use and optimize an already developed high temporal resolution ultraviolet transient absorption spectrometer. Originally, the setup had the capability to generate a pump excitation pulse in the UV range between 260 and 300 nm with sub 25 fs temporal resolution and to probe with a weak pulse in non-perturbative regime from the UV to the visible range. Part of my work involved in extending the probe range to the near infrared a range, covering from 700 to 1500 nm: this allowed me to study the thermalization dynamics of charge carriers in graphene excited out of equilibrium at the saddle point over a broad spectral range of the Fermi-Dirac distribution. Given the excellent temporal resolution of the setup, I could study the dynamics of excited states of light-harvesting complexes. In natural photosynthetic systems the energy flows from various molecules able to capture light to the final reaction centre, where conversion into chemical energy occurs. Every step of the energy cascade is typically faster than the 100 fs timescale, allowing extremely high efficiency. The higher energy photons are absorbed by carotenoids that are incorporated in the photosystem. Such molecules, as beta-carotene, are too complicated to be modelled by ab-initio quantum mechanical simulations. This is not true for the small m5 carotenoid. The number of conjugated bonds (five for such system) has the effect to blue-shift the absorption band but does not influence the photo-physics. In collaboration with a theory group of the University of Bologna, we studied the dynamics of excited states of carotenoids in a conjugated experimental and theoretical effort at the limit of the theoretical capabilities and the experimental resolution. This allowed to understand the processes of carotenoids excited states dynamics with a fully ab-initio quantum theory and confirm it experimentally for the first time. Classical ultrafast spectroscopy employs ultrashort pulses in a high intensity regime that is typically several order of magnitude far from the real conditions where photosystems operate in nature. An experimental investigation closer to that regime has never been performed. During my PhD thesis, I explored the possibility of single-photon time resolved spectroscopy exploiting the quantum nature of light. To explore the field of quantum spectroscopy, I developed a setup to generate pairs of spectrally entangled photons and to fully characterize the joint spectral features. The setup allows exploiting a new degree of freedom in static absorption experiments: entanglement. This could open new insights in light-matter interactions and eventually disclose new physics. As a last project, I developed a time resolved single photon fluorescence lifetime spectroscopy experiment. The technique allows studying samples pumping the molecules with single photons and resolving the excited states dynamics by fluorescent detection. The setup has been used to study a photosynthetic complex from light harvesting bacteria. It was possible to investigate the dynamics of the photosystem in the unprecedent regime of single photon excitation and resolve the dynamics of energy transfer both temporally and spectrally. Such work is a preliminary experiment, and we hope it could pave the way for a new regime in ultrafast spectroscopy with excitation conditions much closer to those occurring in the real world.

MODELING AND DESIGN OF NONLINEAR ALL-DIELECTRIC METASTRUCTURES FOR THZ NANOPHOTONICS

Arregui Leon Unai– Supervisor: Giuseppe Della Valle

Electromagnetic optics has witnessed a rapid and fruitful progress on account of the advanced nanofabrication techniques that have enabled the realization of optical devices with nanometric dimensions, resulting in a transformative switch from diffraction-limited and bulky systems (comprising lenses, digital electronic components...) to flat optical platforms based on compact planar configurations of subwavelength antennas. Simultaneously, numerous commercial software and computational tools have enabled the implementation of sophisticated numerical algorithms for solving the mathematical equations that govern the interaction of light with matter across the entire range of the electromagnetic spectrum. A particularly rich spectral window is the so-called terahertz (THz) region, which overlaps with the characteristic time scales of a vast variety of physical processes including charge carrier dynamics in nanostructures, vibrational modes in organic substances, lattice oscillations in crystals, or intraband transitions in semiconductors. Light waves with THz frequencies are thus a key ingredient to optically probe and exploit these fundamental phenomena, but the high THz atmospheric absorption has supposed a major obstacle in the development of powerful, broadband and tunable THz sources.

In this thesis, all-dielectric nanoantennas are designed and employed as the building blocks of ultrathin THz metasurfaces which, through their effective optical nonlinear susceptibility, are able to efficiently generate THz radiation from a femtosecond optical beam, readily available from table-top lasers operating at the near-infrared (NIR). In fact, the designed semiconductor nanostructures have proved to be a competitive alternative for nonlinear THz nanophotonics over their metallic counterparts, owing to their capability to exploit bulk nonlinearities, reduced material losses in the NIR with respect to those of noble metals, mature fabrication methods and low cost. The proposed semi-analytical and computational modeling approaches demonstrate their validity to describe second-order nonlinear effects in different material platforms such as AlGaAs or $LiNbO_3$. In this spirit, full-wave simulations are combined with concepts from nonlinear optics and electromagnetism, revealing the key ingredients for developing efficient, adjustable and multifunctional THz devices: Mie-type resonances that localize, enhance and spatially redistribute the optical fields within the nano-objects, phonon-enhanced nonlinear susceptibilities, and/or mixed THz light-matter states, known as phonon-polaritons, enrich the near- and far-field response attainable from platforms consisting of the aforementioned optical antennas. As reported in Figure 1, this knowledge is applied to enhance THz generation by nanopatterning thin films as well as to achieve control over the THz emission directionality. In addition, driven by the emergent field of analog optical computing, the potential of polar semiconductors to perform event recognition via THz generation is proved. These findings offer the opportunity to explore, in tight collaboration with experimental research, innovative pathways to uncover novel insights and practical solutions for versatile and scalable next-generation photonic technologies.

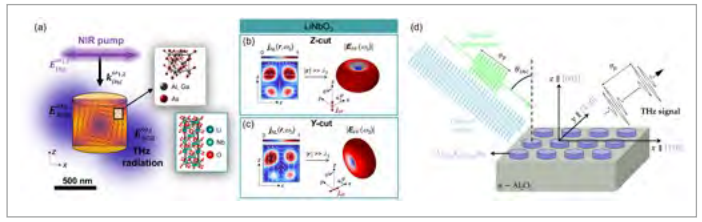

Fig.1 - All-dielectric metastructures for nonlinear THz nanophotonics. (a) High refractive index dielectric nanopillars for efficient NIR-to-THz conversion; the 2D image inside the nanopillar shows the field distribution of the magnetic dipolar Mie resonance. (b)-(c) Tuning of nonlinear THz radiation pattern in $LiNbO_3$ nanoantennas, through the rotation of the crystallographic axes relative to the laboratory frame. (d) Conceptual sketch of temporal edge detection via THz generation with an AlGaAs-on-sapphire metasurface; the optical control signal (blue) is used to perform the time domain derivative of the information signal (green), which is recorded in the nonlinearly generated THz pulse (black).

NANOSTRUCTURED P3HT INTERFACES: UNLOCKING THE POTENTIAL TO INFLUENCE CELL FATE

Anthea Villano - Supervisor: Maria Rosa Antognazza

There is an increasing demand for tools capable of selectively modulating the functions of non-excitable cells with high spatial and temporal precision. Conjugated polymers possess unique physical and optical properties determined by their molecular structure, making them valuable for optically regulating cellular functions. The combination of light stimulation and organic semiconductor technology ensures minimal invasiveness, full reversibility, and the ability to function without an external electrical bias. In particular, poly(3-hexylthiophene-2,5-diyl)(P3HT)-based nanostructured interfaces offer a promising solution for controlling biological activity.
P3HT-based nanoparticles (NPs) in fact act as exogenous, intracellular phototransductors: when stimulated by visible light, they react with oxygen releasing reactive oxygen species (ROS) which turns into a modulation of the behaviour of cells, by altering their membrane potential and/or by affecting their physiological metabolism and redox state.
This research focuses on the production and characterization of three different types of P3HT-based NPs, all of which exhibit good colloidal stability, a hydrodynamic diameter ranging from 50 nm to 300 nm, and a negatively charged surface. These NPs efficiently absorb green light and emit in the red spectrum while supporting charge photo-generation. Additionally, their nanostructured nature makes them particularly effective for interfacing with and adapting to the intricate nanoscale features of living tissues.
The biomedical applications of these NPs were explored in both cardiovascular and epithelial contexts. With increasing life expectancy and aging populations, addressing conditions such as aortic stenosis, vascular regeneration following myocardial infarction, and enhanced wound healing has become a priority.
In cardiovascular applications, both *in vitro* and *in vivo* studies demonstrated the effectiveness of P3HT-based NPs. Selective cell targeting capability was achieved by ad hoc functionalization. *In vitro* and *in vivo* localization of NPs was assessed by confocal microscopy. Importantly, treatment with NPs did not show any sign of toxicity, thus fully confirming the suitability of P3HT-based NPs for chronic *in vivo* use. NPs were delivered to mice and pigs, and in both cases light stimulation protocols were successfully optimized in order to avoid phototoxic damage upon long-term stimulation. *In vivo* NPs photoexcitation induces statistically significant modulation of physiological activity and may represent a breakthrough tool in the treatment of cardiovascular disease.
In the field of epithelial applications, the role of P3HT-based NPs in wound healing was investigated. The wound healing process involves accelerated proliferation, differentiation, and apoptosis of keratinocytes, the predominant cells responsible for the continuous renewal of the epidermis, the outermost layer of the skin. Fibroblasts, which contribute to tissue repair, were also studied. Nanostructured devices based on conjugated polymers responsive to green light were used to promote re-epithelialization of wound sites. A scratch assay was conducted to evaluate the ability of keratinocytes to migrate and close wounds. Cells treated with NPs and stimulated by light exhibited significantly enhanced migration compared to control conditions. Recent results using three-dimensional skin models further confirmed that stimulated NPs significantly modulate cell physiological behaviour, in fully biocompatible operating conditions.
Based on these results, research has progressed toward the development of a more translational tool designed for ease of handling and storage: a biodegradable patch composed of a hydrogel based on a natural polymer integrated with organic NPs. Both NPs-loaded and NPs-free patches were fully characterized. Following biocompatibility verification, mechanical, thermal, rheological and swelling analyses revealed no significant differences between the two patch formulations. The effectiveness of these patches on a skin wound model will be further assessed by examining their impact on wound closure rate and area reduction.
In conclusion, P3HT-based nanostructured devices hold great potential for advancing regenerative medicine.
Their ability to interact with biological tissues in a non-invasive, reversible, and controlled manner makes them valuable tools for therapeutic applications. Future research should focus on optimizing their long-term biocompatibility, fine-tuning their functionalization for specific cell types, and exploring their scalability for clinical applications. With continued development, these nanostructured interfaces may pave the way for innovative treatments in cardiovascular regeneration, wound healing, and beyond.

PRINTED ORGANIC MICRO-THERMOELECTRIC GENERATORS

Stavroula Vovla - Supervisor: Eugenio Cinquanta

While conventional semiconductors have been extensively studied in the literature, with topics like inter- and intra-band transitions, charge injection, and free carrier mobility being accessible through visible light spectroscopies, more complex semiconductors, such as perovskites, require the chemical selectivity provided by XUV spectroscopy. This allows for the study of femtosecond processes, like formation and dissociation of quasi-particles, at the atomic level, unveiling information about their electronic, magnetic, and optical properties.
Such quasi-particles can be large polarons, which are known to hinder carrier recombination and enhance diffusion length in perovskite semiconductors, form on ultrafast timescales. To capture these events, IR pump–XUV probe transient absorption spectroscopy is essential. The experimental setup uses a pump pulse to excite carriers from the valence band to the conduction band, with the pulse wavelength selected based on the material's band gap. A delayed probe pulse then measures transitions from core orbitals to unoccupied states, revealing absorption edges.
For this type of experiments, I commissioned a tabletop experimental line for transient spectroscopy, with IR pulses centered at 800nm and eXtreme UltraViolet (XUV) probe pulses up to 150 eV. The beamline is mainly operated in a transmission configuration, but a study to implement a reflectivity geometry was performed, confirming the compatibility of the two configurations. XUV generation revolves around the up-conversion of IR pulses via High Harmonic Generation (HHG) in a gas-filled hollow capillary. To optimize this process, I used a custom microfluidic device, fabricated by the FAST group of Politecnico di Milano, using the FLICE technique. This device produces an intense, broad, continuous XUV signal which can be used to discern small shifts in narrow absorption edges. Further testing proved that it could transfer the polarization state of the impinging beam to the generated one, which can be an effective tool for the characterization of chiral materials (Figure 1). In this beamline, the output of an amplified Ti:Sapphire laser system is exploited, where 90% of a 35 fs pulse train of 800μJ energy at 1kHz repetition rate is used for XUV generation and 10% acts as the pump beam. The majority of the experimental line is located in a vacuum chamber system, where a pressure gradient is present; from around 10^{-4} mbar at the HHG chamber, due to the injected gas in the microfluidic device, up to 10^{-7} mbar at the spectrometer chamber. The pump and probe pulses are impinging in a non-collinear configuration onto the sample. The sample holder contains space for multiple thin-film samples that can be studied in parallel, as well as a BBO crystal used for achieving spatial and temporal pump-probe overlap. The transmitted or reflected XUV signal is then dispersed by a grazing incidence grating and detected by a Micro-Channel Plate followed by a phosphor screen. The image displayed on the phosphor screen is acquired by a visible CCD camera. The detection scheme also contains an XUV polarimeter based on multiple Fresnel reflections to retrieve the light's Stokes parameters. The use of this polarimeter can lead to a notable signal loss, therefore its use is restricted only for chiral and magnetic materials.
For benchmarking my beamline, I set up a transient absorption experiment on Silicon, whose literature review has been extensive. I targeted the transient evolution of the sharp $L_{2,3}$ absorption edge at ~99eV. The static measurements, seen in Figure 2A, yielded a satisfactory outcome, replicating reported results. For the transient measurements, the Optical Density (OD) of Si was calculated. In this case, OD is defined by the Beer-Lambert Law:

$$OD = -\log_{10}\frac{I_{on}}{I_{off}}$$

where I_{on} signifies the intensity of the transmitted probe signal in the «pump on» state while I_{off} represents the intensity of the transmitted probe signal when the system is in the «pump off» configuration. In Figure 2B, a cumulative measurement consisting of eight ten-minute measurements, spanning -30 ps to 30 ps in 10 ps intervals, is depicted, after applying a Principal Component Analysis (PCA) correction. A negative signal, indicated by the shift from red to blue and back to red along the color scale, is evident around the 99 eV mark. However, no changes in this signal are observed in different details, signifying that its source is a slow phenomenon. Literature suggests a thermal load from pumping pulse, prompting two implemented solutions: a rastering system and reducing the laser system's repetition rate with a mechanical chopper. Rastering cycles the sample through different areas for each delay, reducing exposure time. Decreasing the repetition rate extends thermal load diffusion time.
Utilizing the Si experiment as a reference, we are conducting similar experiments on perovskitic semiconductors. A preliminary feasibility assessment, seen in Figure 3, has indicated that for perovskites with AMX_3 (A: cation, M: metal cation, X: halide anion) stoichiometry, performing transient reflectivity measurements on the available edges of the halogen site are more suitable than transient reflection due to substrate and fabrication limitations. This assessment was also critical in order to estimate the material thickness that optimizes the signal-to-noise. Thus, it was decided that two samples, both produced via evaporation, would be most suitable: $FAPbBr_3$ and $FAPbI_3$ with Br doping. The perovskite samples required for these studies are supplied by the CNST laboratory at the Istituto Italiano di Tecnologia (IIT).

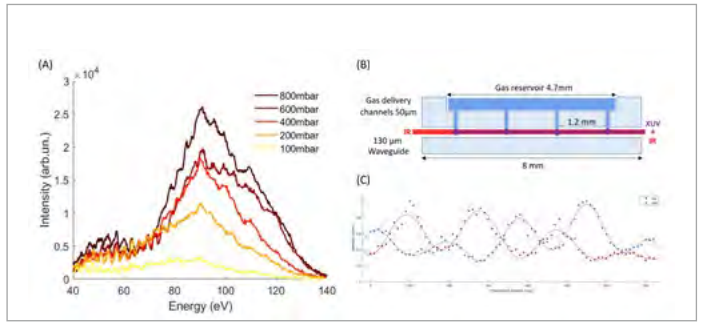

Fig.1 -(A) Generated XUV signal for HHG in He with 800nm driving pulses for various pressures of helium injected in the microfluidic device. (B) Schematic of the microfluidic device. (C) Intensity measurements of the XUV signal in two positions, as a function of the polarization rotation, indicating the transfer of the polarization state of the impinging beam to the generated one.

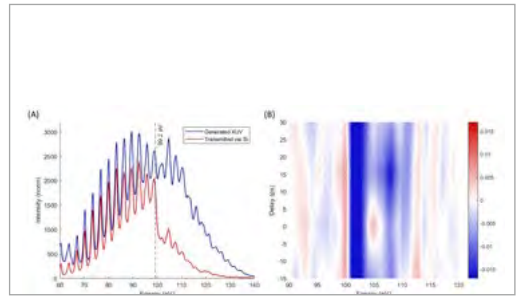

Fig.2 - (A) Comparison of the generated XUV signal (blue) in He for its optimal pressure and the trnasmitted signal through a polycrystalline Si 100nm thin-film indicating the the L2,3 absorption edge at 99eV. (B) Differential absorption map for a cumulative 80 min transient measurement on Si after implementing Principal Component Analysis (PCA).

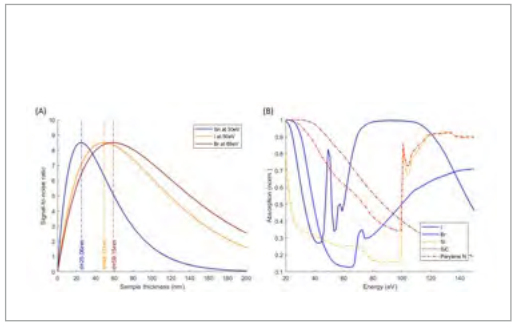

Fig.3- (A) Calculated Signal-to-noise ratio of the ASTRO-FESTA detection scheme for various halogen atoms in their respected absorption edges, indicating their desired sample thickness. (B) Theoretical absorption of possible substrate materials.

STIMULATED EMISSION IN POLYCRYSTALLINE METAL HALIDE PEROVSKITE THIN FILMS

Chun Sheng Wu - Supervisor: Annamaria Petrozza

Lead halide perovskites have gained massive attention in this decade, as their high defect tolerance and low fabrication costs make them a revolutionary material that could replace traditional (III-V / II-VI) compound semiconductor materials. Over the decade, various photonic devices based on perovskites have shown exponential improvement in their device efficiencies. So far, perovskite tandem solarcell have been demonstrated with power conversion efficiency over 29%, light-emitting diodes (LEDs) have achieved a record peak external quantum efficiency (EQE%) of 32%, and X-ray detectors were demonstrated with scalable sizes and low detection limits. Furthermore, these perovskite-based optoelectronic devices are quickly approaching the stage of commercialization. As for lasing applications, although perovskite materials have shown optically pumped lasing with ultra-low threshold and capability to be integrated in different types of cavities, laser diodes based on perovskite semiconductors have yet to be demonstrated.
Most of the groups working on perovskite laser diodes, also have great experiences in high-efficiency LED device development. The underlying operational logic between LEDs and laser diodes is different, and a lack of understanding of stimulated emission mechanism might lead to difficulties during the development of perovskite laser diodes. In this thesis, we unveil the trap-mediated stimulated emission in lead halide perovskites.
We start by investigating formamidinium lead iodide ($FAPbI_3$) perovskite thin films, a state-of-the-art model system for light emitting diodes, where trap density management can be achieved by tuning the FA^+ cation stoichiometry. We show that excess formamidinium iodide (FAI) salt has a role in the passivation of carrier traps, thus on the enhancement of PLQY, especially in low excitation density regimes. However, for high excitation densities close to the amplified spontaneous emission (ASE) threshold condition, we discovered that the threshold increases corresponding to the passivation of shallow traps. By expanding on the three-level system model for stimulated emission, we clarify that the excess FAI salt has a passivation effect on both shallow and deep traps, but for laser applications where the system works at high excitation densities, the shallow trap levels have an affirmative effect for achieving low threshold stimulated emission. Then, we derived a three-level laser rate equation model to quantify the changes in threshold values with respect to carrier dynamics. Our work is to provide a complete model to illustrate stimulated emission processes and evaluate the performance of a perovskite gain medium as a function of its chemical composition, trap nature and thin film morphology. Furthermore, we employed a combination of microscopy techniques to investigate the optical gain mechanism in perovskite thin films. We used fluorescence hyperspectral imaging (HSI) microscopy to monitor the spatial variability of ASE (Amplified Spontaneous Emission). Our analysis revealed that ASE originates specifically from the boundaries of perovskite grains, as observed through correlations between scanning electron microscopy (SEM) and HSI images. Further investigation using photoemission electron microscopy (PEEM) spectra and HSI images showed that these grain boundaries exhibit a higher density of defect states. This suggests that ASE arises from the defect states present at these boundaries.
To delve deeper into this phenomenon, fluorescence lifetime imaging spectroscopy (FLIM) was employed. It revealed that carrier lifetimes are extended in these grain boundary regions, which supports the necessary energy level configuration for establishing a three-level system. Our findings challenge conventional views regarding defects in perovskite materials. While defects are typically considered detrimental due to joule heating in high-current applications, our study underscores their role in achieving optical amplification. This highlights the importance of managing defect density to optimize both optical gain and charge injection efficiency in the development of electrically operated perovskite laser diodes. In conclusion, Organic-inorganic lead halide perovskite material has attracted significant attention in the field of optoelectronic applications. Its intriguing optoelectronic properties show potential in various fields such as photovoltaic technology, sensing devices, X-ray detection, lighting applications, and light amplification. The versatility of this material in adapting to different types of devices is unprecedented, and its applications have achieved significant successes in research laboratories. Furthermore, there is also a gradual increase in the commercialization of perovskites in recent years. Despite the progress in various fields, the development of light amplification in perovskite semiconductors has been limited to the stage of optical pumping, with the demonstration of electrical operation in perovskite laser diodes yet to be achieved. The main challenges are attributed to Joule heating during current injection and a lack of clarity regarding the optical gain mechanisms. The primary focus of this thesis is to uncover the optical gain mechanism using advanced techniques such as ultra-fast spectroscopy, microscopic PL spectroscopy, and electron microscopy. The results of this study are expected to provide valuable insights.

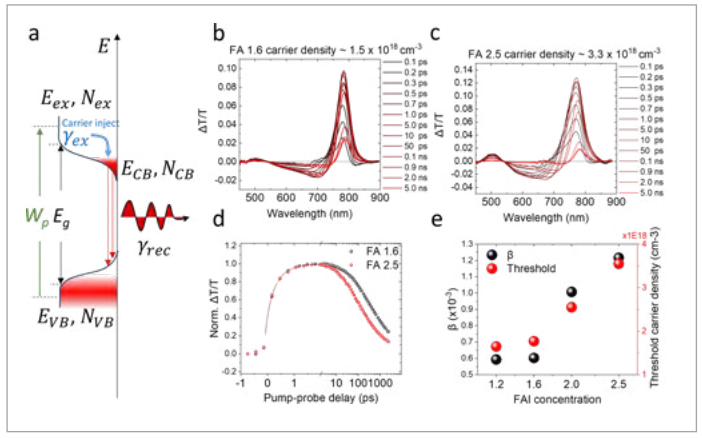

Fig.1 - Relaxation lifetime curve comparison between FA 1.6 and FA 2.5 samples. a) The three-level laser model, the carrier is excited to super-bandgap excited state then relax to band edge in a short time, then accumulated at the band edge. b,c) TA spectra of FA 1.6 and FA 2.5 samples. d) The GSB signal of FA 1.6 and FA 2.5, plotted as a function of pump-probe delay. e) The relation between the lifetime ratio factor β and the ASE threshold carrier density plotted as a function of excess FAI concentration (Excitation wavelength: 670 nm, carrier density: close but below threshold condition, FA 1.6 ≈ 1.5 × 10^{18} cm^{-3}, FA 2.5 ≈ 3.3 × 10^{18} cm^{-3}).

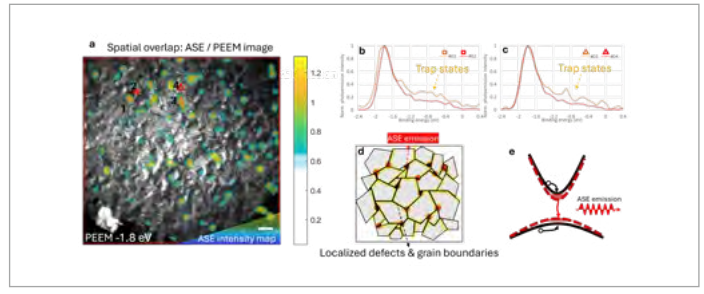

Fig.2 - Spatially correlations between ASE hotspots and thin film morphology. a. Spatial overlap between the ASE intensity map and PEEM image. The rectangle and triangle area represent the selected ROI region. The red ROI stands for intense ASE regions; the cyan represents weak ASE regions. b.c. The PEEM spectra of the corresponding selected areas. The intense ASE regions correspond to regions with higher defect density. d.e. The schematic of ASE mainly originates from localized defects of the grain boundaries. Scale bar = 2 μm.

NON-INVASIVE RECORDING OF CARDIOMYOCYTES' INTRACELLULAR ACTION POTENTIAL VIA ELECTROLYTE-GATED ORGANIC TRANSISTORS

Giulia Zoe Zemignani – Supervisor: Mario Caironi

Excitable cells, such as cardiac cells, neurons, and skeletal muscle cells, rely on action potentials (APs) to encode and transmit crucial physiological information. These electrical impulses result from a rapid and temporary change in the cell's membrane potential, governing essential biological functions such as muscle contraction, synaptic communications and endocrine secretions. In the cardiovascular system, APs play a fundamental role in regulating heartbeat frequency and coordination, ensuring efficient blood circulation throughout the body. Disruptions in AP generation or propagation can lead to severe cardiac disorders, including arrhythmias, heart failure, and sudden cardiac arrest.
The cardiac action potential is a precisely controlled sequence of depolarization and repolarization events, mediated by ion channels that regulate the flow of sodium (Na^+), calcium (Ca^{2+}), and potassium (K^+) ions across the cell membrane. These ion movements generate electrical currents that enable synchronized contraction, ensuring that the heart beats in a coordinated manner. Given its critical role in maintaining cardiovascular health, accurately recording the cardiac AP is of paramount importance in both basic research and clinical applications. High-fidelity electrophysiological recordings allow researchers to investigate the fundamental properties of heart cells, model disease mechanisms, and develop and test new therapeutic strategies. Moreover, the pharmaceutical industry relies on AP measurements to assess the cardiac safety of new drug candidates, as many medications can have adverse effects on cardiac electrophysiology, potentially leading to proarrhythmic or cardiotoxic outcomes.
The patch-clamp technique has long been considered the gold standard for intracellular AP recordings. This highly sensitive method provides precise measurements of ion channel activity and membrane potential changes at the single-cell level. However, despite its accuracy, patch-clamp recording presents several limitations: it is invasive, technically demanding, and has low throughput. The process involves physically inserting a glass pipette into the cell membrane, which often leads to cell damage and limits the duration of recordings. These challenges hinder the use of the technique for large-scale studies or high-throughput applications.
To overcome these drawbacks, alternative non-invasive techniques have been developed. Microelectrode arrays (MEAs) are one such approach, enabling extracellular recordings of cardiac cell activity. However, MEAs primarily detect field potentials (FPs), which lack the detailed APs resolution necessary for precise electrophysiological studies.
To obtain AP recordings, MEAs are often combined with opto- or electroporation techniques, which temporarily porate the cell membrane to enhance signal detection. While this approach improves the fidelity of recordings, it introduces additional complexity, increases costs, and limits long-term measurement capabilities due to the rapid resealing of the cell membrane.
To address these limitations, this thesis explores the use of organic transistors as a novel, non-invasive, and scalable platform for recording APs from cardiac cells. Transistors whose channel is comprised of three different organic semiconductors were coupled with human induced pluripotent stem cell-derived cardiomyocyte (hiPSC-CM) monolayers to assess their ability to capture high-fidelity action potentials. The results demonstrated that, depending on the electrical coupling at the interface between the transistor's channel and the cell membrane, the recorded signals exhibited either AP or FP morphologies. Notably, two of the three tested organic semiconductors successfully enabled AP recordings with high signal fidelity and an excellent signal-to-noise ratio.
To validate the efficacy of this novel platform, AP recordings obtained with organic transistors were directly compared with those from conventional patch-clamp technique and commercial MEAs under similar experimental conditions. The platform demonstrated strong agreement with patch-clamp data, confirming its potential as an effective alternative for accurate electrophysiological measurements. Furthermore, the proposed platform enabled real-time monitoring of drug-induced effects on cardiomyocytes' APs. The device successfully detected subtle waveform oscillations and abnormalities following the administration of cardiovascular drugs, illustrating its ability to provide valuable insights into drug-induced arrhythmias.
These findings establish organic transistors as a transformative technology for electrophysiological studies. The platform offers several key advantages over existing methods, including non-invasiveness, high-throughput capability, and long-term recording stability. By overcoming the limitations of traditional techniques such as patch-clamp and MEAs, this approach has the potential to revolutionize cardiac disease modelling, drug screening, and bioelectronic research.
Beyond cardiomyocytes, this technology could be extended to other excitable cell types, such as neurons, smooth muscle cells, and skeletal muscle cells, enabling broader applications in neuroscience, pharmacology, and regenerative medicine. Future optimization of the materials and device architecture could further enhance recording performance, making this platform even more effective for studying electrophysiological activity in various biological systems.
Moreover, by offering a cost-effective, scalable, and label-free alternative to existing AP recording methods, this platform could significantly accelerate pre-clinical drug testing and regulatory approval processes. Its ability to provide physiologically relevant and high-throughput electrophysiological data could reduce reliance on animal models and improve the predictive accuracy of in-vitro studies, ultimately leading to safer and more efficient drug development pathways. This approach represents a significant step towards the next generation of electrophysiological recording techniques, opening new paths for studying the electrical activity of living cells with unprecedented precision and accessibility.